Intermolecular Interactions

Gunnar Karlström and Bo Jönsson
Department of Theoretical Chemistry
Lund University

February 6, 2013

Contents

List of Figures

List of Tables

1 Introduction

" ... there is also much here that has not been seen, but heard from men of credit and veracity. We will set down things seen as seen, things heard as heard, so that our presentation may be an accurate record, free from any sort of fabrication. And all who hear it may do so with full confidence, because it contains nothing but the truth."

(From Marco Polo, "The Travels")

The intention with the present lecture notes is to give a complete description of intermolecular or interparticle interactions in chemically interesting systems. With "complete" we mean a description that starts on a truely molecular or atomic level dealing with the forces between two molecules in the gas phase. Then we proceed to study the interaction of two molecules in a medium, *i.e.* in a condensed phase. Now the interest will not be focussed on the *energy* of interaction but the *free energy* of interaction. The interaction of *e.g.* two ions in vacuum is a true *pair interaction*, while when the same ions interact in aqueous solution their mutual interaction will be modified by the water molecules. In the latter case we will refer to it as an *effective interaction*. The effective interaction is a free energy of interaction, since we have performed an average over degrees of freedom of the water molecules. For example, it will be temperature dependent. This concept of averaging over certain degrees of freedom will be a recurring theme in these lecture notes. By doing so, we often move from a quantum mechanical to a classical formalism. We will also gradually loose the atomic or molecular picture and treat the system under study on a more coarse grained level, trendy words for this today are "mesoscopic level" or "nanostructures". You have probably already experienced several types of effective models in different chemical contexts. The dielectric continuum model is one example, that also forms the basis for several other familiar descriptions like the Debye-Hückel and Poisson-Boltzmann theories. It should be noted that it is possible to define interaction free energies also for molecules in a very dilute gas phase. We can *e.g.* define the interaction free energy as a function of the separation of two water molecules. This function is obatined by calculating the average over the orientational degrees of freedom of the two water molecules.

To study intermolecular interaction in a chemical system can often lead to heavy numerical calculations in the form of *ab initio* quantum chemical methods or large scale molecular dynamics and Monte Carlo simulations. We will discuss these aspects to some extent, but intermolecular interactions can also be approached on a more descriptive level with a very modest amount of calculations done with paper and pen. The latter is the more fruitful approach for the ordinary chemist.

Intermolecular interactions are of fundamental importance in understanding how atoms and molecules organize in liquids and solids. As an example consider the formation of a micelle from charged surfactant molecules: Why do micelles form and what are the forces acting between the surfactant molecules? Obviously, it is not sufficient to only consider the interaction between the surfactants, because of the trivial fact that micelles neither form in the gas phase nor in a pure surfactant. The solvent plays a crucial role for the micellar aggregation and water is in this respect almost unique. For example, micelles can not form in a solvent with a low dielectric permittivity resulting with only a weak screening of the electrostatic repulsion between headgroups. Can one understand the formation of a micelle based on the knowledge of how surfactants, counterions and water interact? Yes - it can be understood on a qualitative level, but it is not possible to quantitatively predict it from first principles. A related example is the folding of proteins - which are the driving

forces behind the fold and can they be understood as more general forces. The following sections describe in more detail the types of intermolecular interactions, that operate in these systems.

1.1 The molecular size

In the study of atomic and molecular forces one can discard forces whose effects do not coincide with molecular dimensions, *i.e.* gravitational forces are negligible. Only forces with an electric origin, arising from the interaction between electrons and nuclei in different molecules, are of interest for the present applications. At this point it can be appropriate to recapitulate what are the dimensions of small molecules and how strong (in kJ/mol) is a typical hydrogen bond in, for example, aqueous solution. A rough estimate of the size of a water molecule can be obtained from its density,

$$\rho_{H_2O} = 1g/cm^3 \qquad M_{H_2O} = 18g/mol \Rightarrow v_{H_2O} = \frac{M_{H_2O}}{\rho_{H_2O} N_{Avog}} = 30\mathring{A}^3 \tag{1}$$

The volume of a water molecule is approximately 30 $\mathring{A}^3$ and if we treat it as a cube with side length a we get,

$$a^3 = 30 \rightarrow a \approx 3\mathring{A} \tag{2}$$

Thus the average separation between two neighbouring water molecules is approximately 3 Å. This knowledge gives us a chance to estimate the heat of vaporization of water.

The dominant interaction between two water molecules is the dipole-dipole term. Using the known dipole moment of water, 1.85 D, and assuming the average separation between two water molecules to be 3 Å, one finds a typical pair interaction energy to be around -15 kJ/mol. As a comparison we can mention that an accurate quantum chemical calculation would give a value of about -20 kJ/mol. If we assume that water has on the average four neighbours all contributing -15 kJ/mol, we find that the heat of vaporization is of the order of -30 kJ/mol (the factor of two comes from dividing the interaction energy between the two molecules). The experimental value for the enthalpy of vaporization at 373 K and normal pressure is -40.6 kJ/mol. Thus, with these simple calculations we have obtained reasonable numbers deviating less than a factor of two from the true experimental values.

Let us take one more example: what is the dipole moment of acetone? The boiling point of acetone is roughly the same (a little less) than that of water. The boiling point reflects the interaction in the liquid, the pair interaction, so let us equate the pair interaction energy for water and acetone,

$$\frac{\mu^2_{H_2O}}{a^3_{H_2O}} \approx \frac{\mu^2_{acetone}}{a^3_{acetone}} \tag{3}$$

where $a_{acetone}$ can be calculated from the density and molecular weight of acetone. We know μ_{H_2O}, hence we can calculate $\mu_{acetone}$ from eq.(3) giving a value of 3.0 D, which happens to be identical to the experimental value. These rough calculations are of course only presented here in order to encourage the use of approximate estimates when considering intermolecular interactions.

Now let us look a little bit more stringently on the problem and try to find a way in which sophisticated quantum chemical calculations can contribute to the understanding of intermolecular interactions. Assume two atoms or molecules an infinite distance apart. The total energy consists of the individual contributions, *i.e.* the energy of the isolated

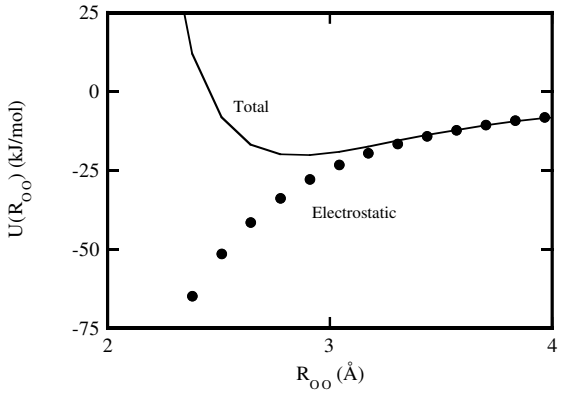

Figure 1: The interaction of two water molecules as calculated in an *ab initio* quantum chemical calculation. The solid line represents the total interaction energy, while the dotted line shows the electrostatic component.

atoms 1 and 2. When bringing them together they will interact and the total energy is given by,

$$E_{tot}(r) = E_1 + E_2 + U(r) \tag{4}$$

$U(r)$ is the intermolecular potential and is defined as the work required to bring two atoms together from an infinite separation to a distance r,

$$U(r) = -\int_{\infty}^{r} F(s)ds \qquad i.e. \qquad F(r) = -\frac{\partial U}{\partial r} \tag{5}$$

where $F(r)$ is the force acting between two atoms/molecules. Since the force is the negative derivative of the potential energy one concludes that a repulsive force is not necessarily associated with a repulsive interaction energy.

Consider an atom consisting of a heavy, positively charged nucleus surrounded by fast electrons able to instantaneously respond to changes in the nuclear positions. The Born-Oppenheimer approximation then states that the potential energy only depends on the relative positions of the nuclei. With this assumption it is possible to numerically solve the Schrödinger equation. In practise this approach is limited to systems including less than approximately 100 electrons. In order to investigate the interaction of larger molecules one can try to divide up the total energy into more manageable contributions and treat them separately. Hopefully the loss in theoretical rigour will be compensated by a deeper insight into the physical nature of molecular forces.

Note that the discussion initially is limited to the interaction between a pair of atoms/molecules in vacuum. This is a true pair interaction, which is independent of solvent and temperature. Later in this chapter the investigation will include the interaction between two molecules in a medium, *e.g.* two ions in water. Their interaction will depend on the dielectric permittivity of the solvent, which makes the interaction temperature dependent. This type of interaction will be referred to as an effective pair potential. and we have to rewrite eq.(5) to include also the entropy. Denoting the free energy with $A(r)$ we have,

$$U(r) - TS(r) = A(r) = -\int F(s)ds \qquad i.e. \qquad F(r) = -\frac{\partial A}{\partial r} = -\frac{\partial U}{\partial r} + T\frac{\partial S}{\partial r} \tag{6}$$

Effective potentials are frequently encountered in chemistry and the hydrophobic interaction and the screened Coulomb interaction are typical examples.

EXERCISES

1. What is the gravitational interaction between two sodium ions at a separation of 3 Å? Compare it to the corresponding Coulomb interaction.

2. How far does a water molecule in liquid water travel on average in one second? How many turns does the same molecule make during the same time? Hint: Diffusion.

3. Give an example of when the entropic force, $T\partial S/\partial r$ is much larger than $\partial U/\partial r$.

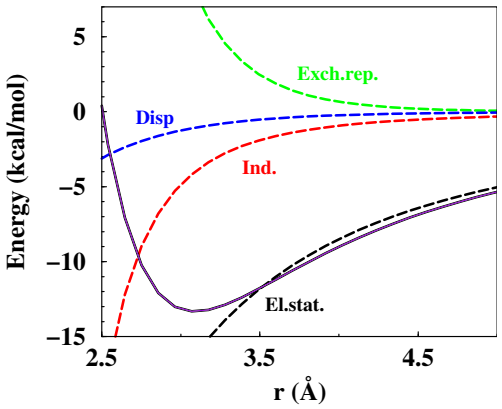

Figure 2: Interaction (kcal/mol) between a water molecule and a chloride ion as a function of distance (solid line). Different energy contributions are shown are shown as dashed lines.

2 The Interaction between two Molecules

In this section we will study the interaction between molecules, starting from a classical point of view. We will find that a large part of intermolecular interactions can be understood without quantum mechanics, but when necessary we must come back to a description of this type. We will start by stating that the total interaction between molecules always can be divided into different terms with a physical meaning according to

$$E_{int} = E_{elstat} + E_{ind} + E_{disp} + E_{exrep}(+E_{mix}) \tag{7}$$

The meaning of the subscripts are interaction, electrostatic, induction, dispersion, exchange repulsion, and a small mixing term, which will be ignored here. (For the weak interactions that we are considering here this is a good approximation, but for stronger interactions the mixing term becomes more important.)

2.1 Electrostatic interaction

The basis of this description of molecules is the charge distribution of the molecules. This charge distribution will be denoted with ρ for an unperturbed molecule and ρ' for the perturbed charge distribution. Formally we may calculate the charge distribution from the electronic wavefunction, $\Psi(r)$, as

$$\rho(r) = \Psi^*(r)\Psi(r) \tag{8}$$

The contribution from the nuclei can easily be added as delta functions afterwards. Using this notation we can write the electrostatic interaction between two molecules as

$$E_{elstat} = \int \rho_1(r_1)\frac{1}{r_{12}}\rho_2(r_2)dv_1dv_2 \tag{9}$$

If the charge distributions of the two interacting systems are overlapping then a complication arises. Different orbitals must be orthogonal according to the Pauli principle. Since the orbitals were optimal before the orthogonalisation, *i.e.* they were choosen to give as low energy as possible, the orthogonalisation will increase the energy. Another consequence of the orthogonalisation is that electrons are removed from the region between

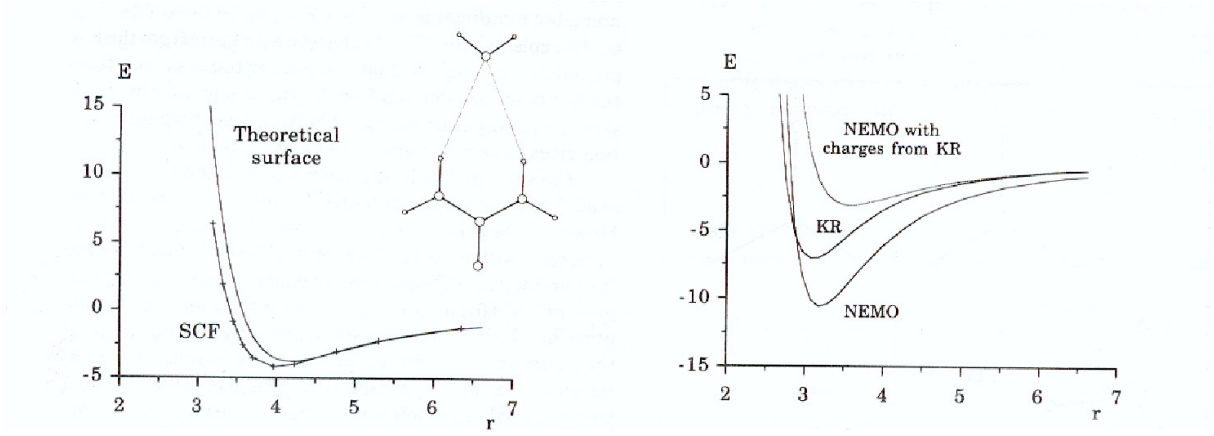

Figure 3: Interaction (kcal/mol)on between a water molecule and an urea molecule. The left figure shows the structure and the SCF and the fitted surface. The right shows the potential obtained when the dispersion is included. A comparison with a potential constructed by Kuharski and Rossky is also included.

the overlapping molecules. We will come back to this issue when we discuss many body interactions.

Every non spherical charge distribution emits an electric field. Thus, when two charge distributions interact, each of them will experience a field from the other. It is the interaction between this field from one charge distribution and the other charge distribution which defines the electrostatic interaction. However, each of the two charge distributions will adopt to the field from the other and we will obtain two polarized charge distributions. As mentioned above, we will denote the perturbed charge distributions with $\rho^{'}$. One would then perhaps believe that one could write the interaction between the two molecules as in eq.(9) but with the perturbed charge distributions. This is not correct since energy is required to change ρ to $\rho^{'}$. We know that the unperturbed charge distributions are optimal, *i.e.* they correspond to a minimum energy. This means that the energy derivative with respect to changes of ρ is 0. The first surviving term will then be quadratic in $\delta\rho = \rho^{'} - \rho$. For small changes of ρ one can show that the following relation holds,

$$E_{ind} + E_{elstat} = \frac{1}{2}\int [\rho_1 \frac{1}{r_{12}} \rho_2^{'} + \rho_1^{'} \frac{1}{r_{12}} \rho_2] dv_1 dv_2 \tag{10}$$

Eq.(10) is accurate enough for the purpose that we will use it for here. The factor 0.5 comes from the fact that half of the polarization energy is spent to modify the unperturbed charge distributions. This is a consequence of that the interactions are weak. There is however a major problem with eq.(10) in that we have not specified any method to calculate the perturbed charge distributions. We will come back to this problem later, but let us first focus on how to calculate the electrostatic and induction interaction between several molecules. To simplify the equations we will introduce the notation $E_{elstat}(1,2)$ for the electrostatic interaction between molecule 1 and 2 according to eq.(9). Using this notation one can write the total electrostatic interaction between molecules 1, 2 and 3 according to,

$$E_{elstat}(1,2,3) = E_{elstat}(1,2) + E_{elstat}(1,3) + E_{elstat}(2,3) \tag{11}$$

The electrostatic interaction is additive as can be seen from this equation. With additive we mean that it is equal to the sum of all pair interactions. Consequently it is easy to write an equation for the total interaction between N molecules.

$$E_{elstat}(1\ldots N) = \sum_{n=1}^{N}\sum_{m<n}^{N} E_{elstat}(n,m) = \frac{1}{2}\sum_{n=1}^{N}\sum_{m\neq n}^{N} E_{elstat}(n,m) \tag{12}$$

Our next task is to examine the properties of the induced interaction when many particles are present. This will be slightly complicated and we start by examining the induced interaction between two particles. From eqs.(9) and (10) one easily obtains,

$$E_{ind} = \frac{1}{2}\int [\rho_1 \frac{1}{r_{12}}(\rho_2^{'} - \rho_2) + \rho_2 \frac{1}{r_{12}}(\rho_1^{'} - \rho_1)] dv_1 dv_2 \tag{13}$$

The first term corresponds to the energy gain due to polarization of molecule 2 by the presence of molecule 1, whereas the second term comes from the opposite polarization. The first impression one gets from this equation is that the induction energy is linear in the polarization of the two molecules. This is however not correct. Let us assume that the charge distribution associated with system 1 cannot be polarized and is made up from *e.g.* a proton in some position in space. The second term in eq.(13) is then identically 0. The integration of the first term of $dv1$ becomes unnecessary, since the proton is located to a point, and we are supposed to evaluate and integrate the product of the potential of ρ_1 and the charge density difference $\rho_2^{'} - \rho_2$ over dv_2. This difference is naturally also linear in the potential from ρ_1. Thus, the response is quadratic in this potential. As we will see below one normally uses the field from the molecules when estimating the integral and naturally the result will be also quadratic in these fields. Below we will use atomic units in order to simplify the expressions and avoid $4\pi\epsilon_0$ as much as possible. The atomic units have their origin in quantum chemistry and are chosen to make equations simple. Thus the charge of the electron is 1., the Bohr radius (the radius of the electron orbit in the Bohr model for the hydrogen atom) is 1. and also $4\pi\epsilon_0$ is choosen to be 1. For those who are not familiar with these units, the following relations may be useful:

Length 1 a.u. = 0.52917 Å
Charge 1 a.u. = The charge of an electron
Energy 1 a.u. = 627.52 kcal/mole =2625 kJ/mole
Dipole moment 1 a.u. = 2.54 Debye
Polarizability 1 a.u. = 0.52917^3 $Å^3$

Let us now introduce a multipole expansion of the charge distributions of the interacting molecules. A natural way to do this is to consider two molecules A and B which are so far apart that their charge distributions do not overlap. When the distance between A and B is larger than the molecules, then it is fruitful to expand the charge distribution of the molecules in a multipole expansion. The first term in this expansion is the charge of the molecule, the second term the dipole and the third term the quadrupole moment.

$$q = \sum_i q_i \tag{14}$$

$$\mu_x = \sum_i q_i x_i \tag{15}$$

$$\Theta_{xx} = \frac{1}{2}\sum_i q_i x_i^2 \qquad\qquad \Theta_{xy} = \frac{1}{2}\sum_i q_i x_i y_i \tag{16}$$

The expansion is infinite, but for practical purposes it is normally enough to truncate the expansion after the dipole, quarupole or octupole term depending on the system. It should be noted that only the unique components are specified above. Since this type of expansion is central to our understanding of intermolecular forces it will be given some consideration. Consider a set of point charges e_i each located at $\mathbf{r}_i = (x_i, y_i, z_i)$ describing molecule A. We will now calculate the potential at a point P due to the charges e_i - see Figure 4. It is important that P is further away from the origin than all points $\mathbf{r}_i$.

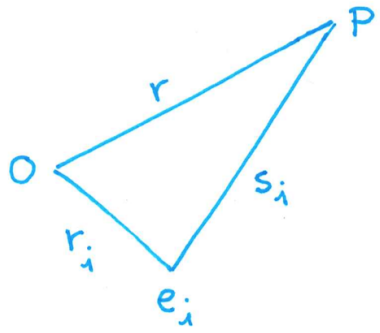

Figure 4: Geometric arrangement.

The potential at point P due to the charges e_i is given by,

$$\phi(P) = \sum_i \frac{q_i}{s_i} \tag{17}$$

First we note that the equations are given in atomic units, thus we avoid cumbersome constants. It is now convenient to write $\frac{1}{s_i}$ in a Taylor series,

$$\frac{1}{s_i} = \frac{1}{r} + x_i\frac{\partial}{\partial x}(\frac{1}{r}) + y_i\frac{\partial}{\partial y}(\frac{1}{r}) + z_i\frac{\partial}{\partial z}(\frac{1}{r}) + \frac{1}{2}[x_i^2\frac{\partial^2}{\partial x^2}(\frac{1}{r}) + x_i y_i\frac{\partial^2}{\partial x \partial y}(\frac{1}{r})\ldots] \tag{18}$$

Here we note that the differentiation should be evaluated at the origin of the charge distribution. If eq.(18) is inserted into eq.(17) one obtains for the potential at point P.

$$\phi(P) = \sum_i q_i \left(\frac{1}{r} + x_i\frac{\partial}{\partial x}(\frac{1}{r}) + y_i\frac{\partial}{\partial y}(\frac{1}{r}) + z_i\frac{\partial}{\partial z}(\frac{1}{r}) + \frac{1}{2}[x_i^2\frac{\partial^2}{\partial x^2}(\frac{1}{r}) + x_i y_i\frac{\partial^2}{\partial x \partial y}(\frac{1}{r})\ldots]\right) \tag{19}$$

The sum of the first term, $q = \sum q_i$, defines the potential due to the total charge of the system if it was placed at the origin, where q is the total charge in the system. Note that this q is exactely the same as was defined in eq.(14). In a similar way we may identify the components of the dipole moment in the next three terms, which are the dipole moment components defined according to eq.(15).

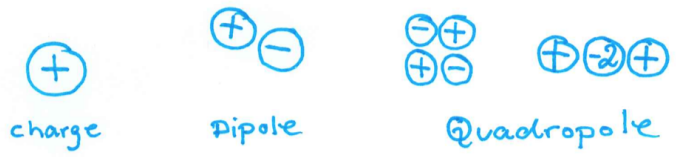

Figure 5: Schematic representation of charge, dipole and quadrupoles.

The quadrupole moment components are then defined by the next terms which are identical to what is specified in eq.(16). These definitions of the quadrupole moment components differs from those normally used. In the notation by Buckingham all elements are multiplied by 3/2 and 1/3 of the sum of q_{xx}, q_{yy} and q_{zz} (the trace of the quadrupole moment matrix) is subtracted from these terms. For a real molecule the sums in the equations above must be replaced by an integral over the charge density of the molecule. In Figure 5 a set of charge distributions corresponding to a charge, a dipole and a quadrupole are shown. It is important to note that the lowest non zero moment is uniquely defined, but that higher moments depend on the choice of origin. To illustrate this we study the charge distribution of a cyanide ion (CN^-). Let us for the sake of simplicity assume that the bond length is 2.0 a.u. and that the entire charge is located to the nitrogen atom. Assume further that we place the cyanide ion along the x-axis with the carbon atom in the origin. The x-component of the dipole moment will then be 0.0*0.0+ 2.0*-1.0 = -2.0 a.u. If we instead translate the ion so that the nitrogen is in the origin and the carbon atom has an x-coordinate of -2.0. For this geometry we obtain a dipole moment of 0.0*-2.0 - 1.0*0.0 =0.0. We see that the translation of the ion has changed the dipole moment with the product of this translation and the ionic charge. See also exercise 6 in this chapter. Eq.(19) defines the potential in the point P, and by differentiating the potential with respect to the position one gets the field and field gradient at the point. Thus, if both charge distributions are represented by multipole expansions, evaluated around O and P, then it is possible to evaluate the total electrostatic interaction energy as a sum of interactions between charge-charge, charge-dipole, dipole-charge, dipole-dipole, charge - quadrupole, quadrupole - charge and so on. If we look at eqns. 15–16 we see that the dipole moment has the dimension charge×length and the quadrupole moment has the dimension charge×length×length. This is also reflected in the energy expressions. Using atomic units energy has the dimension charge×charge/length. Below expressions are given for the first terms in the expansion,

$$E(q_a, q_b) = \frac{q_a q_b}{r_{ab}} \qquad \text{charge} - \text{charge} \qquad (20)$$

$$E(q_a, \boldsymbol{\mu}_b) = -\frac{q_a \boldsymbol{\mu}_b \mathbf{r_{ab}}}{r_{ab}^3} \qquad \text{charge} - \text{dipole} \qquad (21)$$

$$E(q_b, \boldsymbol{\mu}_a) = -\frac{q_b \boldsymbol{\mu}_a \mathbf{r_{ab}}}{r_{ab}^3} \qquad \text{dipole} - \text{charge} \qquad (22)$$

$$E(\boldsymbol{\mu}_a, \boldsymbol{\mu}_b) = \frac{\boldsymbol{\mu}_a \boldsymbol{\mu}_b}{r_{ab}^3} - 3\frac{(\boldsymbol{\mu}_a \mathbf{r}_{ab})(\boldsymbol{\mu}_b \mathbf{r}_{ab})}{r_{ab}^5} \qquad \text{dipole} - \text{dipole} \qquad (23)$$

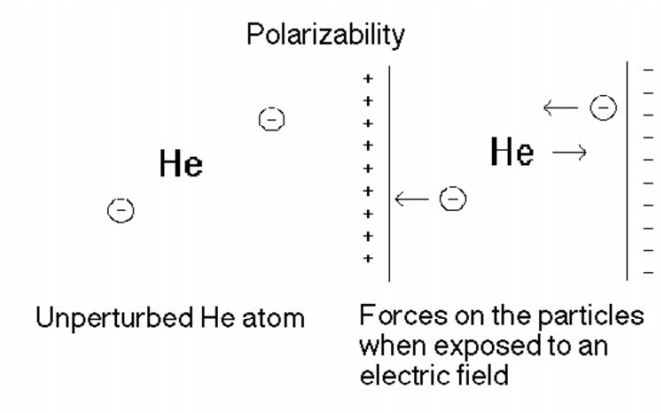

Figure 6: Illustration of how the forces from an externally applied field act on the Helium nucleus and the electrons in a Helium atom.

2.2 Induction interaction

We will now introduce the concept *polarizability*. If we investigate the variation of the total energy, E of a molecular system when an external homogeneous field, f, is applied, it is possible to write the total energy as a power series in the applied field. One obtains the following expression,

$$E(f) = E_0 - \boldsymbol{\mu}_0\mathbf{f} - \frac{1}{2}\mathbf{f}\boldsymbol{\alpha}_0\mathbf{f} + \text{ higher order terms} \tag{24}$$

The first term on the right hand side is the unperturbed energy, the second term the interaction between the molecular dipole moment μ_0 and the applied field, and finally the third term the interaction between the applied field and the rearrangement in the charge distribution. This term is characterized by the polarizability tensor, $\boldsymbol{\alpha}_0$, and is quadratic in the applied field. We will call it the induction energy. The subscript 0 indicates that the properties should be evaluated at zero field. For an isotropic system we may write,

$$E_{ind} = -\frac{1}{2}\alpha f^2 \tag{25}$$

The molecular dipole moment in the presence of the field can be written,

$$\boldsymbol{\mu} = \boldsymbol{\mu}_0 + \boldsymbol{\alpha}_0\mathbf{f} \tag{26}$$

Thus, we can see that the polarizability relates the changes in the molecular dipole moment to the applied field. There naturally exists similar terms which relates changes in the molecular quadrupole moment to the applied field gradient and so on. For small molecules it is normally enough to consider the first term in this expansion.

EXERCISES

4. What is the interaction between two ions with charge +1, when separated by 5 a.u.? 1 a.u. in energy corresponds to 627.5 kcal/mole or 2625.5 kJ/mole. 1 a.u. in length =0.52917 Å. Answer: 1/5 a.u. = 525.1 kJ/mole

5. How big is the maximum and minimum interactions between a charge +1 and a unit dipole, when separated by 5 a.u.? Which are the corresponding orientations? Answer. 1/25 a.u. = 105.0 kJ/mole. Parallel and anti parallel to the vector between the ion and the dipole.

6. Sketch how the interaction between two dipoles varies with the orientation. a) Assume dipole A to be parallel to the vector between the two dipoles. b) Assume dipole A to be perpendicular to the vector between the two dipoles.

7. a) How big is the maximum stabilization between two dipoles separated by 6 a.u. (close to 3 Å the water-water distance in liquid water)? A water molecule has a dipole moment of 0.8 a.u.. b) How big is this interaction at 5 a.u. and at 10 a.u.. The strength of the water - water hydrogen bond is close to 20 kJ/mole for a distance of 3 Å. Answer. a)-.00593 a.u. = -15.6 kJ/mole.

8. Calculate the maximum field from a water molecule 6 a.u. away. (Hint use the results from Ex. 4). Calculate the induced dipole moment and the induction energy caused by this field with a polarizability of 15 a.u.. Answer: The field = 0.0074 a.u. The induced dipole moment = 0.111 a.u. The induction energy = 0.0004 a.u. = 1.1 kJ/mole

9. Assume that we have a dipole located at the coordinate 10,0,0 and the dipole moment is 1.a.u. You are now supposed to calculate the quadrupole moment when origin is used as expansion center. (Hint replace the dipole with two charges.)

It is now time to study the properties of the induction interaction for a many particle system. When a system contains many polarizabilities that interact with each other and with some field, then it is slightly complicated to evaluate the induction interaction in the system. This will be illuminated with an example. Assume that we have two polarizabilities (α=10 a.u.) placed along the z-axis 5 a.u. from each other. On this system we apply an external electric field of 0.001 a.u. in the z-direction. We shall now calculate the induced dipole moment and the induction energy for this system. The simplest way of solving this problem is to use an iterative procedure. We start this by calculating the induced dipole moment for each of the polarizabilities due to the external field. In the first iteration we obtain $\mu_{ind} = 10. * 0.001 = 0.01$ a.u. for each of the polarizabilities. In the next iteration we calculate the field from one of the polarizabilities on the other polarizability. This field equals $2\mu_{ind}/r^3$, where r is the distance between the polarizabilities (5.a.u.). From this we obtain the induced field 0.00016 a.u. on the two polarizabilities. The total field is thus 0.00116 and from this we may calculate new induced dipoles. We obtain $\mu_{ind} = 0.0116$ a.u.. We can continue to iterate and finally we obtain $\mu_{ind} = 0.011905$ a.u.. The same result can naturally be obtained in a more direct way if we realize that the two induced dipoles are equal in size and parallel to the applied field. The following relation can then be written down,

$$\mu_{ind} = \alpha(E_{ext} + \frac{2\mu_{ind}}{r^3}) \tag{27}$$

This equation can easily be solved and one obtains $\mu_{ind} = 0.011905$ a.u. as above. The induction energy can now be calculated from the following formula.

$$E_{ind} = -\frac{1}{2}\mathbf{f}_{ext}\boldsymbol{\alpha}\mathbf{f}_{tot} = -\frac{1}{2}\alpha\mathbf{f}_{ext}\mathbf{f}_{tot} \tag{28}$$

The first equality is a general equation and the second holds for spherical polarizabilities (f_{ext} is the external field). In the general case the external field should be augmented by

the field from all permanent charges, dipole, and so on. f_{tot} is the sum of these external fields and the field from all induced dipoles. This relation can be shown to be exact. Thus, we obtain an interaction between the applied field and the two polarizabilities of $E_{ind} = -2 * 1/2\mathbf{f}_{ext}\boldsymbol{\mu}_{ind}$ =0.000011905. This value is 19 per cent larger than the corresponding value obtained if the coupling between the two polarizabilities was not considered (0.00001).

EXERCISES

10. Carry out similar calculations to the one described above, but where the field is applied perpendicular to the vector between the two polarizabilities.

11. Calculate the interaction energy between two parallel dipoles, each with a polarizability of 15 a.u.. The dipoles are 6 a.u. apart and parallel with the inter dipolar vector. The magnitude of the dipoles are 0.8 a.u.

12. Consider an ion with charge +1 surrounded by 6 octhaedrically coordinated dipoles with the dipole moment 1 a.u.. The dipoles point towards the ion and have each a polarizability of 10 a.u. The ion - dipole distance is 4.0 a.u. Calculate the induction interaction.

13. Consider an infinite chain of parallel dipoles. The polarizability of a particle is 10 a.u. and the dipole moment is 1 a.u. The distance between the particles is 5 a.u. Each dipole points along the chain. Calculate the induction interaction. From these examples we can clearly see that the induction energy is not pairwise additive.

As seen from the examples above, the total induction energy is of the order of 10 - 20 per cent of the electrostatic interaction for a pair of ordinary polar molecules. For a condensed system however it may be even larger (30 -40 per cent see below). The major part of the polarizabilities originates from a redistribution of the electronic cloud around the nuclei, but for polyatomic systems a smaller contribution to the total polarizability comes from changes in bond lengths and angles of the molecules. This latter contribution is normally of the order of a few per cent of the total polarizability.

2.3 Dispersion interaction

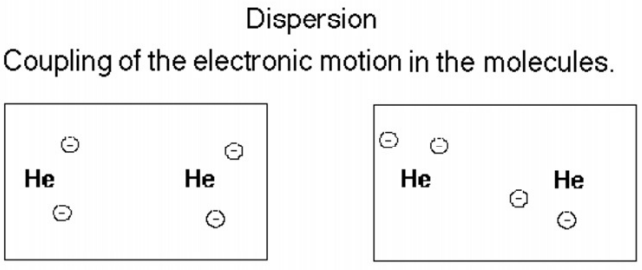

Figure 7: Classical analogue to the dispersion interaction. Note that the electrons belonging to the different He atoms try to avoid each other.

So far we have focused on the electrostatic and induction interactions. These two terms can both be understood in terms of classical electrostatics. The next two terms, however needs a quantum mechanical description, but to the first of them a classical analogue can

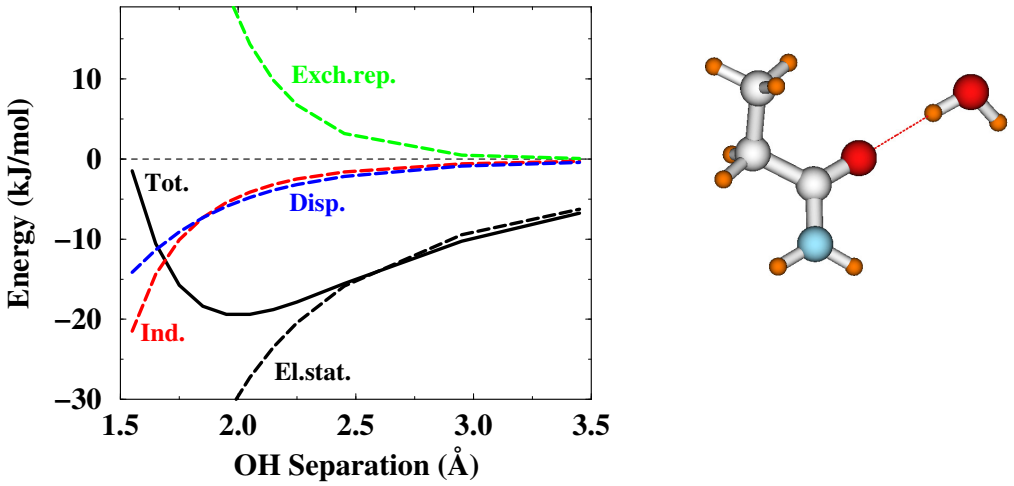

Figure 8: The water-propylamide as a model system for the hydrogen bond to a peptide backbone. Note that the minimum energy is almost the same as for a water-water hydrogen bond, *cf.* Fig. 1.

be imagined. To do so we start by considering two helium atoms. Due to the rotation of the electrons around the nuclei, each of the atoms at a given instance emit an electric field. This field fluctuates rapidly and the atoms have no permanent dipole moment but an oscillating one. The two dipoles couple and this results in an attractive interaction. The interaction is called dispersion interaction (or London dispersion interaction after London, who was the first to explain the phenomenon). London derived the following expression for this interaction,

$$E_{disp}(a,b) = -\frac{3}{2}\frac{1}{r_{ab}^6}\alpha_a\alpha_b\frac{I_aI_b}{I_a+I_b} \tag{29}$$

In this equation I means the ionisation potential of a molecule and α the polarizability as before. Note that the distance dependence is r^{-6}, similar to that of the dipole - induced dipole interaction.

The problem with the non additivity of the dispersion energy has been treated in a classical publication by Axilrod and Teller. From this publication one can deduce that the induction energy is not completely additive. If one assumes that the interacting particles are small and randomly distributed in space, then one can show that the third order correction to the dispersion energy is repulsive with 8 per cent. The correction will be smaller for larger particles.

2.4 Exchange repulsion

The exchange repulsion can, like the dispersion interaction, only be understood from a quantum mechanical model. The simplest way to get a feeling for the physics is to consider two Helium atoms and use an orbital description of their wavefunctions. The Pauli principle states that there can only be two electrons in each orbital. When the atoms come close to each other, the orbitals start to overlap, *i.e.* the electrons are to some extent in the same orbital. This forces the orbitals to change. The change is associated with an energy cost and leads to a repulsion between the atoms.

We will now briefly discuss the many body effects on the exchange repulsion energy. In order to simplify the discussion we will use the fact that the exchange repulsion energy to

a good approximation is proportional to S^2, the square of the overlap between the orbitals of the interacting molecules. To get an insight into the many body effects on the exchange repulsion we will consider three interacting molecules (A,B and C). We will assume that each molecule only have one occupied orbital and that A overlaps with B and C, but that we can ignore the overlap between B and C. We will denote the orbitals on the atoms with a,b and c. Thus, S_{ab} is the overlap between orbitals a and b. The Pauli principle states that the different orbitals must be orthogonal. We can achieve this goal by orthogonalising a to b according to,

$$a^{'} = \frac{a - S_{ab}b}{\sqrt{1 - S_{ab}^2}} \tag{30}$$

where the denominator guarantees that the new orbital is normalized. We note now that the coefficient for orbital a in this orbital is slightly larger than 1. Thus, the overlap between this new orbital and orbital c will be slightly larger than the overlap between the unperturbed orbitals a and c. One can easily calculate the difference and one sees that an extra term $S_{ab}^2 S_{ac}^2$ appears. In physical terms, one may say that the surrounding molecules are confining the electron cloud of molecule A to a part of the space, which increases the exchange repulsion. Apart from these rather complicated and important many body effects there also exists coupling terms of many body nature. *E.g.* if a dipolar molecule is bound to a positive ion then the positive end of the dipole will have less electrons than a free molecule. This will give a smaller exchange repulsion between molecules that binds to the positive end of the dipole. The opposite is true for negative ions.

2.5 The hydrogen bond

We have several times mentioned hydrogen bonds in the text. They have a special place in chemistry. One main reason for this is their intermediate strength. They are much weaker than ordinary chemical bonds, but they are much stronger than the thermal energy kT. This means that they can contribute to the formation of structures (ice and other hydrogen bonded crystals, proteins but also structured liquids as water). A common idea in the litterature is that the hydrogen bond is some sort of intermediate between an ordinary covalent bond and a normal intermolecular interaction. There is however no reason to assume this. An ordinary intermolecular partitioning scheme such as the NEMO model, which will be described below is quite capable of describing this. In Figure 9 the different components to the total interaction energy for the water dimer is shown as a function of the O - O separation. From this figure it is clearly seen that the major stabilising energy contribution is the electrostatic energy but that there are significant contributions from both induction and dispersion. The exchange repulsion energy is rapidly increasing at shorter distances.

2.6 Charge transfer

This is another type of interaction, that is commonly mentioned in physical chemistry textbooks. In the partitioning scheme presented above it appears as a induced interaction but the polarized electrons on molecule 1 are polarized into the virtual orbitals of molecule 2 or vice versa. There is a fundamental problem with this type of interaction since a large

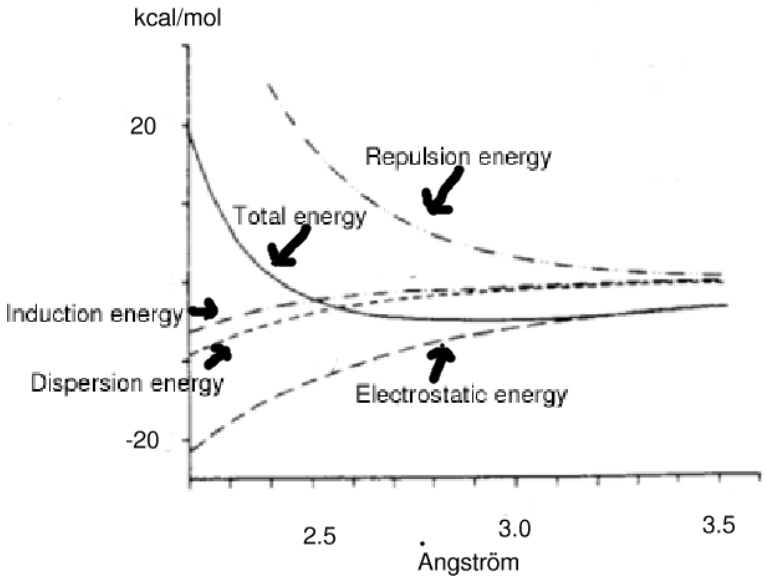

Figure 9: The different energy contributions to the interaction energy for the water dimer as a function of the O-O distance.

part of this effect is due to what is normally called the Basis Set Superposition Error (BSSE), which is a technical complication appearing in quantum chemical calculations. One must thus be careful when charge transfer interactions are discussed in quantum chemical calculations.

There are however systems where a real charge transfer interaction is of importance. This type of interaction can be expected to occur in systems where there are low lying unoccupied orbitals. An excellent example is the complex formed between BF_3 and NH_3. In BF_3 there is on empty low lying orbital originating from one of the 2p-orbitals on the B atom. This orbital is empty since there is only 6 electrons available for the B atom. However this orbital can be used to stabilize the lonepair in the NH_3 molecule. This leads to a relatively strong interaction (around 100 kJ/mol).

2.7 Modelling of intermolecular interactions

The purpose of the previous section was to give insight into the physics behind the interaction between molecules. Of course there are many reason to study the interaction between molecules, but the main reason is probably that the properties and phase behaviour of condensed phases entirely depend on such interactions. Many methods have been developed to study these phenomena, but we will not discuss them here. They all, however, have a common feature that the results that they predict never is more reliable than the potential functions that are used in modelling. Today there exists in the literature four major potential function libraries, GROMOS, AMBER, OPLS and CHARMM. Their standard structure is more or less the same. The interaction between two molecules is described as the interaction between the atoms in the molecules. To each atom a charge is assigned, and the electrostatic interaction between the molecules is calculated as the interaction between these charges. Furthermore, to each pair of atoms, one in each molecule, a Lennard - Jones potential is assigned.

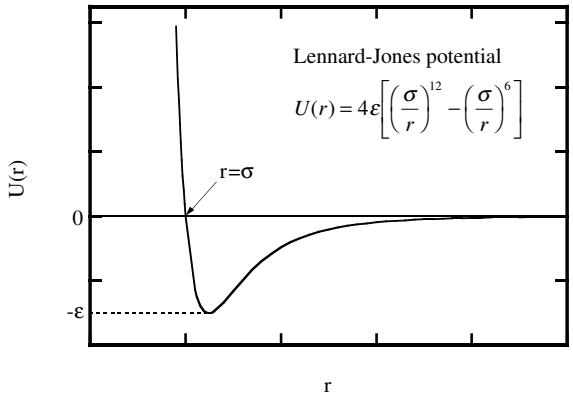

Figure 10: The Lennard-Jones potential.

$$U_{LJ}(r) = 4\epsilon[(\frac{\sigma}{r})^{12} - (\frac{\sigma}{r})^{6}] \tag{31}$$

In this potential ϵ defines the well depth and σ the distance where U_{LJ} equals 0. The latter follows directly from eq.(31), while in order to show the former we have to take the derivative of $U_{LJ}(r)$ wth respect to r,

$$\frac{\partial U_{LJ}}{\partial r} = 4\epsilon[-12\frac{\sigma^{12}}{r^{13}} + 6\frac{\sigma^{6}}{r^{7}}] = -24\epsilon\frac{\sigma^{6}}{r^{7}}[2\frac{\sigma^{6}}{r^{6}} - 1] \tag{32}$$

The derivative in eq.(32) is zero when $r/\sigma = 2^{1/6} \approx 1.12$. Fig.10 shows the functional form. The r^{-6} term describes the dispersion energy and the r^{-12} the exchange repulsion. A typical potential between two molecules A and B is a sum of Coulomb terms and Lennard-Jones terms,

$$U_{AB} = \sum_{i=1,i_A}\sum_{j=1,j_B} 4\epsilon_{ij}[(\frac{\sigma_{ij}}{r_{ij}})^{12} - (\frac{\sigma_{ij}}{r_{ij}})^{6}] + \frac{q_i q_j e^2}{4\pi\epsilon_0 r_{ij}} \tag{33}$$

It is frequently necessary, in particular for systems with strong intramolecular hydrogen-bonds, to consider also the valence bond angles and the bond lenghts in a molecule. The variation of these parameters are small and it is enough to model them with a Hook's law expression U=k*x^2, where x measures the deviation from the optimal value for the-valence bond angle or the bond length. The potentials in the GROMOS, AMBER, OPLS and CHARMM libraries are thus true pair potentials and no many body interactions are present. The quality of the potentials are rather poor and minimum energies can be off by several units of kT and similarly the exchange repulsion can give erroneous volumes. Electrostatic interactions are often badly treated and it is not unusual to introduce *ad hoc* screening factors into the Coulomb term of eq.(33).

The different schemes differ mainly in the parameters used to describe the atoms. The strategy used to determine these parameters is very non-formalistic. Basically a lot of empirical data and some quantum chemical data are used to determine the parameters. Since the amount of empirical data normally decreases with system complexity, the reliability of the potential functions decreases similarly. There are also problems directly connected to the choice of potential form. These can be clearly seen if the water-water potentials are investigated. If the nuclei are used as sites for the charges that models the

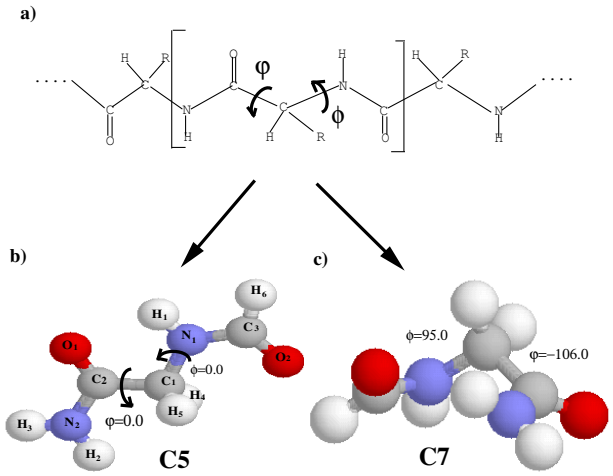

Figure 11: Schematic and space filling models of formylglycine in its two forms (the C5 and C7 structures).

electrostatic, there is only one free parameter to vary and this means that the molecular dipole moment completely determines the electrostatic description of the molecules. The description which is obtained within this approximation is rather crude and one normally uses a set of extra sites, in order that one should be able to model both the dipolar and quadrupolar properties of a water molecule. The same problem naturally occurs for more complex systems, but for these systems there are not enough empirical information to determine the additional parameters needed.

An alternative approach is the use a partitioning scheme as described starting with eq.(14) together with multicenter multipole expansions of the charge distributions and the polarizabilities of the interacting molecules. Using standard electrostatics and the multicenter expansions it is possible to calculate the electrostatic and induction interactions as well as the dispersive interactions using the equations previously given in this text. The NEMO model is one such approach and below we will compare the results obtained with that model with one of the most used empirical potentials and with some quantum chemical calculations. When large and flexible molecules are modelled additional problems arises. First of all knowledge about the dihedral potential for the flexible molecule is needed. Second, when a flexible molecule changes its conformation its charge distribution is changed. In the standard procedures GROMOS, AMBER, OPLS and CHARMM this effect is ignored, and it is assumed that the charge distribution is independent of the molecular conformation. This is in some way consistent with the assumption that the molecules in these models lack polarizability. Several groups have recently started to model these effects in a similar way as we model the intermolecular induction effects. Thus, each atom in the flexible molecule is polarizable and is polarized by the field from other atoms in the molecule. There are problems connected with this approach, that originates from the fact that the field from the atoms next to the considered one can not be included. To illustrate the accuracy (inaccuracy) of the empirical potentials and also potentials like NEMO we will present some results for formylglycine and its complexes with a water molecule. The formylglycine molecule is presented in Fig.11. The two forms presented in the figure are

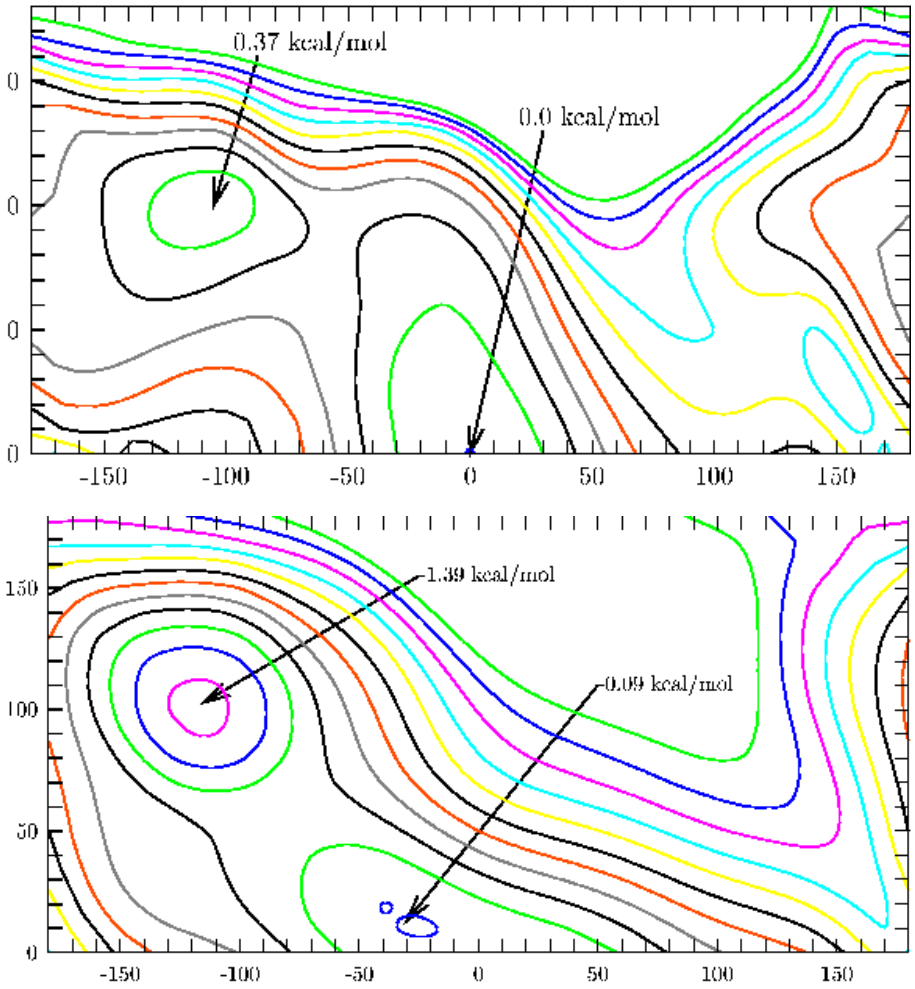

Figure 12: Figure showing the variation of the energy for the formylglycine molecule as a function of the dihedral angles. Other geometry parameters are optimized. Upper: NEMO force field and Lower: AMBER force field

labeled C5 and C7 since a 5- and a 7-membered ring is present in the two structures. As is indicated in the figure there are two bonds around which there are large dihedral flexibility.

In Figs.12 we present the dihedral potentials obtained with the NEMO model and the AMBER model. There are large diferences between the two potentials. The NEMO potential localizes the global minimum to the C5 structure whereas AMBER suggests that the C7 structure is most stable. The total difference in stability between the different structures amounts to 1.8 kcal/mol or close to 3 kT. One can also note that the C5 structure is a saddle point in the AMBER model. Accurate quantum chemical calculations places the C7 structure 0.5 kcal/mol above the C5 structure. The corresponding energies for the CHARMM, OPLS, MM3 and MMFF models are -4.55, -0.37, -0.64 and -1.08 kcal/mol.

Fig.13 presents relative stabilities for some of the complexes formed between a water molecule and formylglycine. The energies for the different structures are given relative the most stable structure for the NEMO model. The energy is set to 0 for all models for this structure. It is obvious that the relative stability is not reproduced from one model to an other. It is difficult to have any opinion about what the correct values are. Thus, the

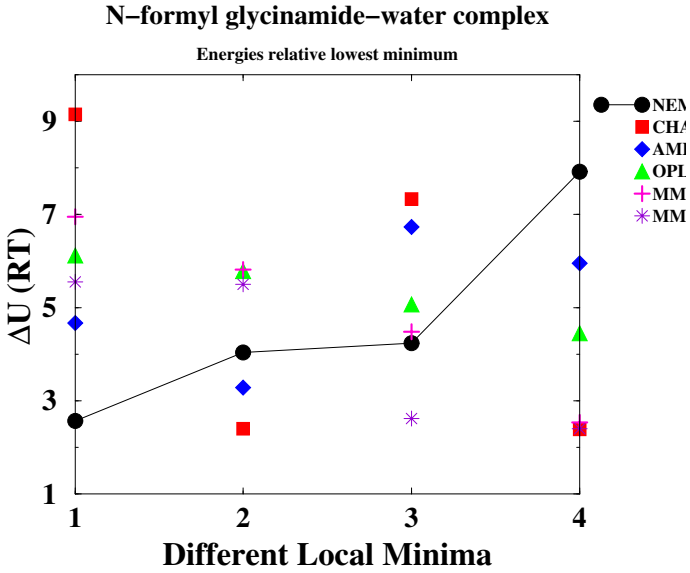

Figure 13: Relative stability of different stable complexes formed between formylglycine and a water molecule. The energy of the most stable form is set to zero.

use of parametrized intermolecular potentials for the interaction between large molecules is not as exact as one could anticipate and the whole area of atomistic macromolecular simulations is more related to belief and hope than to science. Still, with small rigid molecule very accurate results can be achieved. A different maybe more hopeful attitude is to assume that the detailed interactions are not so important as long as the molecular connectivity is correct, that is the covalent bonds are properly in place, and the atoms have a reasonable size. In addition, a small non-specific attractive interaction can be handy. Of course, with such an approach, we are not allowed to ask to detailed questions!

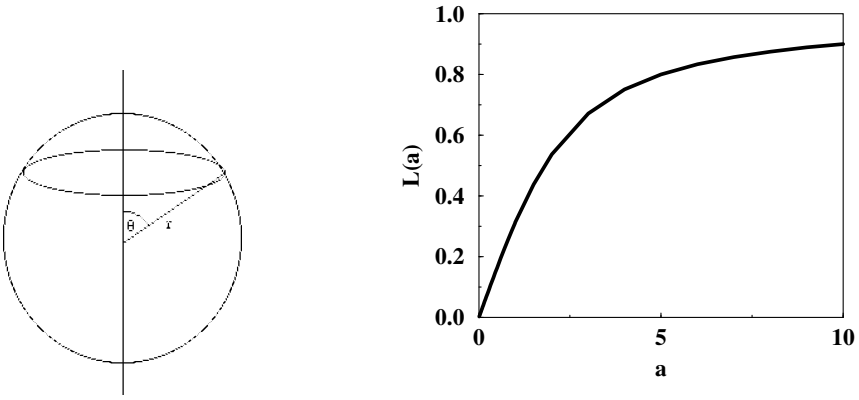

Figure 14: a) Definition of the angle relative the external field. b) The Langevin function.

3 The Effective Interaction between two Molecules

A basic assumption in everything we have said so far has been that we have full knowledge of the relative position and conformations of the interacting molecules. This is a situation which may be relevant for the interaction between molecules in gas phase. The purpose of this section is to develop models which can be used to describe the effective interaction between two molecules in the presence of other molecules, or more generally the interaction of two, or more, species where some degrees of freedom have been averaged out. Formally we can write this interaction as,

$$\beta w(\mathbf{R}^N) = -\ln \int d\mathbf{r}^n \exp[-\beta U(\mathbf{R}^N, \mathbf{r}^n)] / \int d\mathbf{r}^n \tag{34}$$

This describes the free energy of a $N+n$ particle system, where we have averaged out the n particles. This is a completely general procedure in probability theory. That is, asking for a probability of the N objects irrespectively of the n other objects. **Hint:** Compare with the outcome of two coins that are thrown!

3.1 The Langevin model

Before starting to analyze the effective interaction between two molecules it is appropriate to study the interaction between an electric field and a dipole that is free to rotate. There are two features of the Langevin model that are worth noting. First of all it introduces the effective interaction (between an electric field and a dipole) in a clear way, Moreover it introduces the concept saturation in a natural way. We will in the following sections frequently used the dielectric approximation and replaced the influence of the media molecules with a dielectric permitivity. A fundamental assumption in the dielectric approximation is that the response of the medium is linear in the applied field or perturbation. This means that the response to an ion with charge 2 is twice the response to an ion with charge 1. However for larger charges (2 and 3) the medium is not capable to respond linearly on small distances. The Langevin model gives a molecular explanation for this phenomena. Under such circumstances one obtains what is called dielectric saturation. The first step in the development of this model is to consider a free dipole and calculate the probability that it forms an angle θ with an externally defined direction. With the notations in Fig.14a one obtains,

$$p(\theta)d\theta = \frac{2\pi sin\theta r^2 d\theta}{4\pi r^2} = \frac{1}{2}\sin\theta d\theta \tag{35}$$

When a field that can orient the dipole is applied a Boltzmann weighting factor must be added. $-\mu F\cos\theta$ is the interaction between the field an the dipole for a given orientation.

$$p(\theta)d\theta = A\exp(\beta\mu F\cos\theta)\frac{1}{2}\sin\theta d\theta \tag{36}$$

where A is a normalization constant and F the applied field. One easily obtains,

$$A^{-1} = \int_0^\pi \exp(\beta\mu F\cos\theta)\frac{1}{2}\sin\theta d\theta \tag{37}$$

From these equations one can easily calculate the effective or mean interaction between the field and the dipole, and one obtains,

$$U_{mean} = -\mu F\frac{\int_0^\pi \cos\theta\exp(\beta\mu F\cos\theta)\frac{1}{2}\sin\theta d\theta}{\int_0^\pi \exp(\beta\mu F\cos\theta)\frac{1}{2}\sin\theta d\theta} \tag{38}$$

The ratio between the two integrals is the mean value of $\cos\theta$ which can be simplified according to

$$<\cos\theta>=\frac{\int_0^\pi \cos\theta\exp(\beta\mu F\cos\theta)\frac{1}{2}\sin\theta d\theta}{\int_0^\pi \exp(\beta\mu F\cos\theta)\frac{1}{2}\sin\theta d\theta} = \frac{e^a+e^{-a}}{e^a-e^{-a}} - \frac{1}{a} = \text{cotanh}(a) - \frac{1}{a} = L(a) \tag{39}$$

where $a = \beta\mu F$. For small arguments a, $L(a)$ behaves as $\frac{a}{3}$. The interpretation of this is that when the interaction between the field and the dipole is small compared to kT, the thermal energy, then the dipole behaves as a polarizability,

$$\alpha_{eff} = \frac{\mu^2}{3kT} \tag{40}$$

which is the same as the dipole polarizability in eq.(53) apart from the trivial factor $4\pi\epsilon_0$. In a similar way one can show that when the interaction between two dipoles is weak compared to kT then their effective interaction varies in the same the dispersion interaction, *i.e.* as $1/r^6$. In fact one gets an expression which is similar to eq.(29) and where the ionisation potential replaced with $4kT$. If the actual calculation is performed one obtains,

$$G(r,T) = -\frac{\beta\mu^4}{3r^6} + \frac{7\beta^3\mu^8}{450r^{12}} - \frac{133\beta^5\mu^{12}}{33075r^{18}} + \ldots \tag{41}$$

When the interaction is much larger than kT, then the effective interaction approaches a distance dependence of $1/r^3$, similar to the interaction between orientated dipoles. If we assume that the interaction between two molecules can be written as $E(\Omega_1,\Omega_2,r)$ then the thermally averaged interaction for a given distance r can always formally be written as,

$$E_{eff}(r) = \frac{\int_{\Omega_1}\int_{\Omega_2} E(\Omega_1,\Omega_2,r)exp(-\beta(\Omega_1,\Omega_2,r))d\Omega_1 d\Omega_2}{\int_{\Omega_1}\int_{\Omega_2} exp(-\beta(\Omega_1,\Omega_2,r))d\Omega_1 d\Omega_2} \tag{42}$$

3.2 Orientational dependence of polar molecules

3.2.1 Ion-dipole interaction

The interaction between an ion of valency Z and a dipole, μ, can be written as,

$$U_{id} = \frac{Ze}{4\pi\epsilon_0}\frac{\boldsymbol{\mu}\mathbf{r}}{r^3} = \frac{Ze\mu\cos\theta}{4\pi\epsilon_0 r^2} \tag{43}$$

where $\cos\theta$ is the angle between the dipol moment vector and the vector connecting the ion with the dipole, see Fig. 15a. Let us now calculate the effective, or Boltzmann weighted, interaction between an ion and a rotating dipole. Rewriting eq.(34) for the present situation,

$$\beta w_{id}(r) = -ln\int d(\cos\theta)\exp(-\frac{\beta Ze\mu}{4\pi\epsilon_0 r^2}\cos\theta)/\int d(\cos\theta) \tag{44}$$

The integral is easy to solve noting that $\cos\theta$ goes from +1 to -1. Let us also introduce a strength parameter as $\gamma = \beta Ze\mu/4\pi\epsilon_0$. The effective potential then reads,

$$\beta w_{id}(r) = -ln\frac{\exp(\gamma/r^2)-\exp(-\gamma/r^2)}{2\gamma/r^2} \approx -\frac{\gamma^2}{6r^4} \tag{45}$$

Note that the curves in Fig.15 corresponds to an interaction in vacuum. The interaction between an ion and a dipole in aqueous solution will be significantly weaker due to the dielectric screening of the solvent.

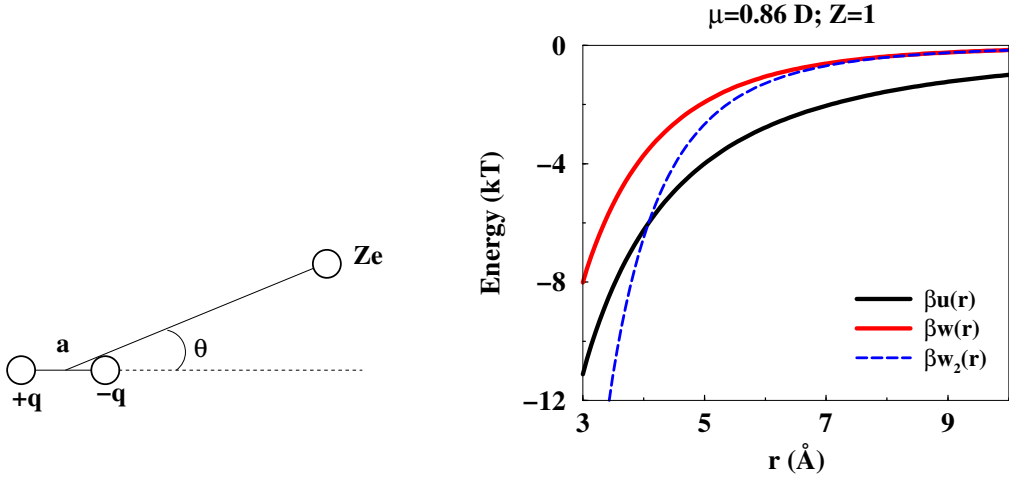

Figure 15: a) The arrangement of a charge Ze and a dipole represented by two charges q and $-q$. b) The orientationally averaged ion-dipole interaction. $\beta w(r)$ is the exact free energy of interaction, while $\beta w_2(r)$ comes from a series expansion to second order of the exact expression. The maximal interaction energy for a colinear arrangement is also shown.

3.2.2 Dipole-dipole interaction - The Keesom term

Let us consider the interaction of two dipoles, which in vector notation can be written as,

$$U_{dd} = \frac{1}{4\pi\epsilon_0}[\frac{\boldsymbol{\mu}_1\boldsymbol{\mu}_2}{r^3} - 3\frac{(\boldsymbol{\mu}_1\mathbf{r})(\boldsymbol{\mu}_2\mathbf{r})}{r^5}] \tag{46}$$

Eq.(46) can also be written in terms of three angles: θ_1 and θ_2 are the angles between the dipole vectors and the vector connecting the two dipoles and ϕ is the dihedral vector formed by the two dipole vectors and the connection vector. Then we obtain the following expression,

$$U_{dd} = \frac{\mu_1\mu_2}{4\pi\epsilon_0 r^3}(\sin\theta_1 \sin\theta_2 \cos\phi - 2\cos\theta_1 \cos\theta_2) \tag{47}$$

From these equations we see that the dipole-dipole interaction is angular dependent and rotating one of the dipoles 180 degrees changes the interaction from repulsive to attractive or vice versa. The attractive interactions will be given a higher weight by the Boltzmann factor with the result that an angular averaged dipole-dipole interaction will be attractive (note, that there is both an average free energy of interaction and an average energy of interaction). Let us start by deriving the angular averaged free energy of interaction. That is, keep r fixed while integrating over the relevant angles, collectively denoted by Ω,

$$\beta w_{dd}(r) = -\ln \int d\Omega \exp(-\beta U_{dd}(r,\Omega))/\int d\Omega \tag{48}$$

where we also have introduced the variable $\beta = 1/kT$ with $k = 1.38010^{-23}$ J/K being the Boltzmann constant. kT is the important measure of energy. A little bit drastically we can say that whenever the important interactions in a system is much larger or much less than kT it is easy to predict the properties. These limits correspond a crystal or an ideal gas, which we know how to handle. When the important interactions are of the order of kT, however, we typically have a liquid. Note that $N_{Avog}kT = RT$, where R is the gas constant. The integral in eq.(48) has no analytical solution and in order to proceed we have to linearize the exponential,

$$\exp(-\beta U_{dd}(r,\Omega)) \approx 1 - \beta U_{dd}(r,\Omega) + \frac{[-\beta U_{dd}(r,\Omega)]^2}{2} - ... \tag{49}$$

In order for the expansion to be valid $\beta|U_{dd}(r,\Omega)| << 1$ and then we can also expand the logarithm accordingly, $\ln(1+x) \approx x$. Integrating the linear term gives zero but the quadratic term gives

$$\beta w(r) \approx \beta w_2(r) = -\frac{\beta^2\mu_1^2\mu_2^2}{3(4\pi\epsilon_0)^2 r^6} \tag{50}$$

Note that the angular averaged *energy* is twice the *free energy* in eq.(50),

$$< \beta U_{dd}(r) >= \frac{\int d\Omega \beta U_{dd}(r)\exp(-\beta U_{dd}(r,\Omega))}{\int d\Omega \exp(-\beta U_{dd}(r,\Omega))} \approx -\frac{\int d\Omega [\beta U_{dd}(r)]^2]}{\int d\Omega} = 2\beta w_{dd}(r) \tag{51}$$

The extra factor of "2" in the energy expression simply comes from the fact that it is the first order term that contributes to the energy, while the second order term is the leading one for the free energy. Since $w(r) = U(r) - TS(r)$, one immediately finds that the entropy of interaction of two dipoles is repulsive. This seems natural as the closer they come the more is an aligned arrangement of the dipoles favoured and alignment leads to a loss of entropy.

Another way to approach the factor of two is by noting that,

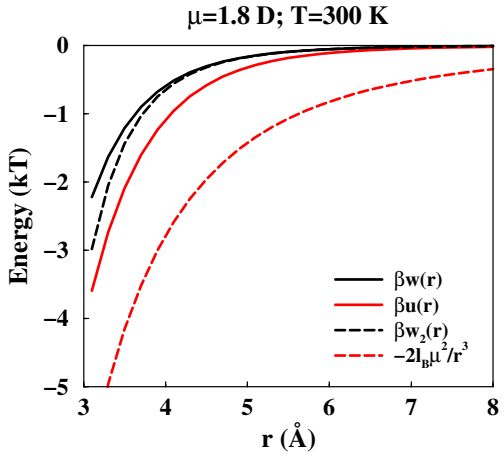

Figure 16: The orientationally averaged dipole-dipole interaction. $\beta w(r)$ is the exact free energy of interaction, while $\beta w_2(r)$ comes from eq.(50). The thermally averaged energy $\beta < u(r) >$ is also included together with the interaction energy for two perfectly aligned dipoles, $-2l_B\mu^2/r^3$.

$$< U >= \frac{\partial \beta w}{\partial \beta} = 2w \tag{52}$$

where in the second step we have used eq.(50).

When is the linearization allowed? Fig.(16) gives an indication of when eq.(50) can be used and when the full expression, eq.(48) must be considered. An unexpected result from Fig.(16) is that $w_2(r) \approx w(r)$, despite the fact that the dipole-dipole interaction between two dipoles with $\mu = 1.8$ D at a separation of 3 Å is several kT. Note also that $w_2(r)$ in eq.(50) varies like r^{-6}, the same distance dependence as the dispersion interaction. The similarity can be made even more close if we define a classical dipole "polarizability" $\alpha^{dd} = \beta\mu^2/12\pi\epsilon_0$ and write the free energy of interaction as,

$$\beta w_2(r) = -\frac{3\alpha_1^{dd}\alpha_2^{dd}}{r^6} \tag{53}$$

The thermally averaged dipole-dipole interaction is usually referred to as the *Keesom interaction.*

3.2.3 Dipole-induced dipole interaction - The Debye term

We know from previous discussions that all molecules have an electronic polarizability. This means that a molecule with a permanent dipole moment, like water, will polarize a nearby molecule,

$$U_{did} = -\frac{\mu^2\alpha}{(4\pi\epsilon_0 r^3)^6}(1 + 3\cos^2\theta) \tag{54}$$

In the same way as in the previous section this interaction can be thermally averaged and for two dipolar and polarizable molecules the resulting interaction keeping only the leading term reads,

$$\beta w_2^{ind}(r) = -\frac{\beta\mu_1^2\alpha_2 + \beta\mu_2^2\alpha_1}{4\pi\epsilon_0 r^6} = -3\frac{\alpha_1^{dd}\alpha_2 + \alpha_2^{dd}\alpha_1}{r^6} \tag{55}$$

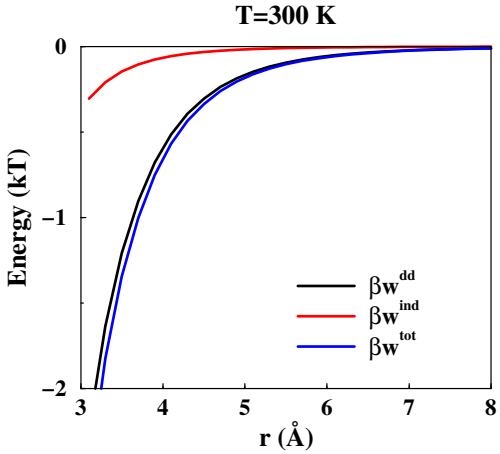

Figure 17: The orientationally averaged dipole-dipole and dipol-induced dipole interaction. βw^{dd} is the exact free energy of interaction for two permanent dipole with $\mu = 1.8$ D, while w_2^{ind} is the corresponding free energy for polarizable dipoles with $\alpha = 1.5$ Å^3. βw^{tot} is the sum of the two terms. The values of μ and α are chosen in order to mimick two water molecules.

Fig.(17) shows the relative importance of the permanent dipole moment and the induced dipole moment for a system roughly corresponding to two water molecules. Note that the induced term is significantly smaller than the permanent one. The linear approximation for $w_2^{ind}(r)$ is essentially exact.

The thermally averaged induced dipole-dipole interaction is often called the *Debye interaction*. The Debye, Keesom and quantum mechanical dispersion interaction all have the same distance dependence and are often lumped into one term referred to as the *van der Waals interaction*. We will repeatedly come back to this very important interaction.

$$\boxed{\text{van der Waals} = \text{Debye} + \text{Keesom} + \text{London}}$$

Other types of orientationally averaged interactions can of course be derived. For example, the interaction between an ion and a dipole is very strong and usually dominates the behaviour of ionic solutions together with the direct ion-ion term. For anions, and in particularly for atoms not belonging to the first and secod row of the periodic table, the ion-induce dipole and dipole-induced dipole terms can be of importance.

3.3 How to define the size of a molecule

What is it we are showing when we draw a space-filling model of a molecule? For a tennis ball it is clear what is meant and the same for a car or a house. The best answer to the original question is probably: repulsive interactions. For a neutral molecule we can even be so specific as to say that it is the *exchange repulsion* or *overlap repulsion*. This analogy between molecules and billiard balls might be useful, but we have to remember that it has limitations. In general, structural information helps our understanding of a system, but is often less useful when it comes to evaluating forces between molecules.

Consider for example the interactions of the three pairs: Na^+-Na^+, Na^+-Cl^-, and Cl^--Cl^-. It is clear that a sodium ion sees another sodium ion as a very large object. The same is true for the chloride ion pair, while a sodium ion sees a chloride ion as a rather small object, because of the Coulombic attraction. Thus, we must not always believe

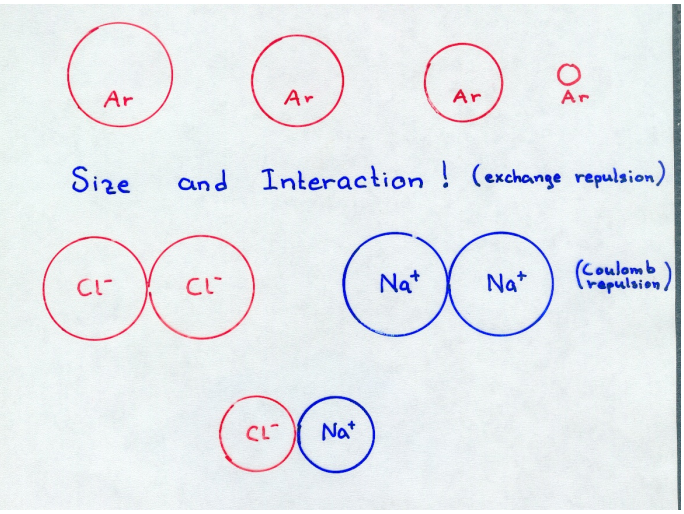

Figure 18: How can we define a size of an argon atom? When the interaction of two argon atoms is equal to ? kJ/mol? The size is obviously related to the interaction and one can define the diameter of a chloride ion as the separation when the interaction between two chloride ions is kT. One problem is that the Cl^- diameter will then be different if we consider the interaction Na^+ - Cl^-! As a matter of fact it will be much more different than the figure indicate.

in the so-called lock-and-key mechanisms of interaction frequently used in biochemistry - they rely on the assumption that long range interactions are absent.

Let us take an illustrative example of how difficult it is to determine a "molecular size". A reasonable way to define the size is to say that the diameter of two identical molecules is equal to the separation where their mutual interaction is equal to kT. Taking two Ar atoms we find an approximate radius of 3 Å. For two sodium ions we run into a problem, because the Coulomb interaction is long ranged,

$$u_{++}(r) = \frac{e^2}{4\pi\epsilon_0 r} \approx kT \Rightarrow r \approx 550\mathring{A} \tag{56}$$

With the same choice of repulsive limit as in the argon case we get the ridiculous result above. Thus, the conclusion must be to proceed with some care in charged systems. (The size calculated in the example above is often used in the liquid theories and it is then referred to as the "Coulomb hole". In many respects, it has the same properties as the hard core of an argon atom). Fig.(18) and (19) are meant to illustrate the complexity with the "molecular size" concept. Thus, the lock and key idea might be applicable in the absence of long range interactions, but can lead completely astray when electrostatic interactions are present giving a significant contribution to the total interaction.
Textbooks in physical chemistry usually present a lot of different molecular radii, but one should remember that they are all operationally defined. Of course, they can be useful, but they do not have the quantitative accuracy one might imagine from the large tables and all the decimals. One molecular radius has in our opinion a larger relevance than several others and that is the radius obtained from the liquid density and the molecular weight,

$$R = (\frac{3M}{\rho N_a 4\pi})^{1/3} \tag{57}$$

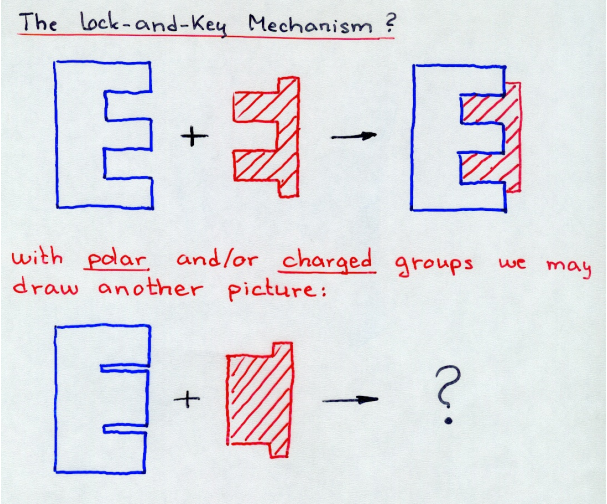

Figure 19: The lock and key mechanism with short range and long range interactions. Which picture is most relevant?

Let us take water as an example: $M = 18$ and $\rho = 1g/cm^3$, which gives a radius of 1.9 Å. Compare this number with the oxygen-oxygen radial distribution function in Fig.27.

Tabulated radii are sometimes useful as relative measures. Compare *e.g*:

- $F^- = 1.36$ $Na^+ = 0.95$; $Cl^- = 1.81$ $K^+ = 1.33$
- $Na^+ = 0.95$ $Mg^{2+} = 0.65$ $Al^{3+} = 0.50$
- $F^- = 1.36$ $Cl^- = 1.81$ $Br^- = 1.95$ $I^- = 2.16$
- Ne = 1.54 Ar = 1.88 Kr = 2.01 Xe = 2.16

3.3.1 Repulsive model potentials

The exchange repulsion, which we normally associate with the molecular size is very short ranged or steep. We do not know the exact mathematical form, but for many purposes is it enough with a hard sphere potential. Below are a few forms given:

- Hard sphere potential, $u(r) = \infty$ for $r < \sigma$ - mathematically and conceptually convenient
- Power law potential, $u(r) \propto r^{-n}$ with $n > 0$ - mathematically convenient
- Exponential potential, $u(r) \propto \exp(-r/\sigma_1)$ with $\sigma_1 > 0$ - physically most correct

Note that one can not combine a repulsive exponential potential with an attractive power law, like in eq.(58).

$$u_B(r) = B\exp(-r/\sigma_1) - \frac{C}{r^6} \tag{58}$$

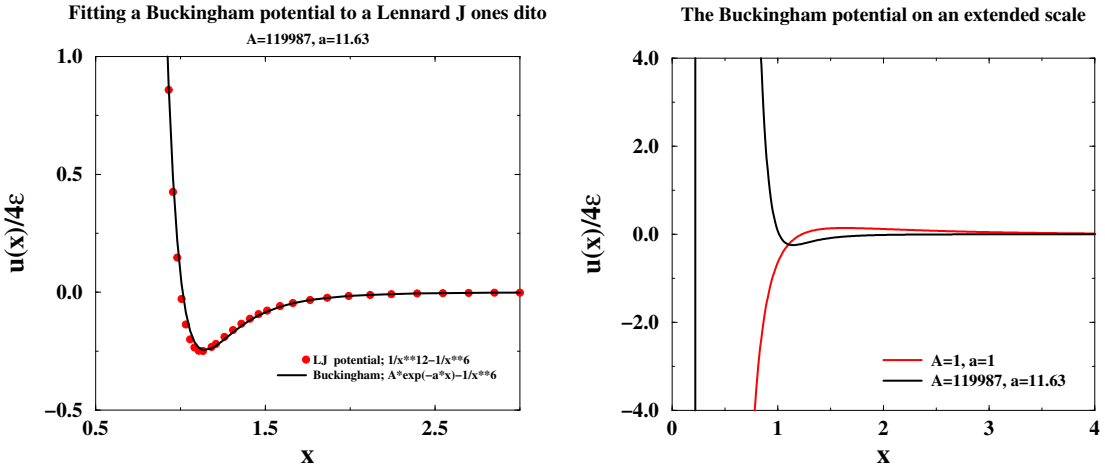

Figure 20: a) Fitting the Buckingham potential to an LJ potential over a limited interval b) The complete Buckingham potential over a larger interval illustrating the divergence for small arguments. Note that the existence of the divergence is independent of the parameters A and a.

Let us compare a Lennard-Jones potential to the so-called Buckingham potential, eq.(58). What happens for small r? Under which circumstances does it play a role? We make the simplification that $C = 4\epsilon$ and it also helps to introduce the scaled variable $x = r/\sigma$. We might then proceed to fit the Buckingham potential to the LJ potential determining the parameters $A = B/4\epsilon$ and $a = \sigma/\sigma_1$.

$$\frac{u_{LJ}(x)}{4\epsilon} = \frac{1}{x^{12}} - \frac{1}{x^6} \tag{59}$$

$$\frac{u_B(x)}{4\epsilon} = A\exp(-ax) - \frac{1}{x^6} \tag{60}$$

Performing a least-squares fit one obtains the following numbers: $A \approx 119987$ and $a \approx 11.87$ if the fit is constrained to the interval around the LJ minimum - see Fig.(20a). The complete Buckingham potential is of course divergent for small x as can be seen in Fig.(20b).

3.4 Second virial coefficient

So far we have analyzed the effective interaction between two molecules for a fixed intermolecular separation. One can however proceed one step further and define a measure of the effective interaction between two molecules. Normally this is done in terms of the *second virial coefficient*, B_2. Let us start by making a virial (series) expansion of the pressure,

$$\beta p = \rho + B_2(T)\rho^2 + B_3(T)\rho^3 + \ldots \tag{61}$$

where ρ is the particle density. If all coefficients $B_i = 0$ then we obtain the ideal gas law (*i.e.* non-interacting particles), hence the second, third ... virial coefficients contain information about intermolecular interactions. It is a straigthforward exercise to derive the formal expressions for B_i and for example the second virial coefficient is defined as,

$$B_2(T) = -\frac{1}{2V}\int_V [\exp(-\beta u(\mathbf{r}_1, \mathbf{r}_2, \mathbf{\Omega}_1, \mathbf{\Omega}_2) - 1] d\mathbf{r}_1 d\mathbf{r}_2 d\mathbf{\Omega}_1 d\mathbf{\Omega}_2 \tag{62}$$

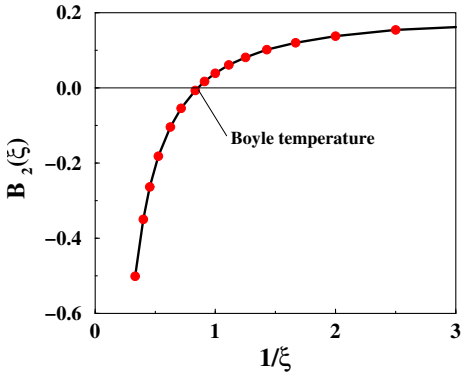

Figure 21: The second virial coefficient for a Lennard-Jones gas drawn as a function of the dimensionless parameter $\xi = 4\beta\epsilon$, which is inversely proportional to the temperature.

The equation can be simplified if we assume that we have an isotropic system of spherical particles. Under these conditions we obtain,

$$B_2(T) = -2\pi \int_0^\infty [\exp(-\beta u(r)) - 1] r^2 dr \tag{63}$$

where $r = \mid \mathbf{r}_1 - \mathbf{r}_2 \mid$. Thus, repulsive interactions will give a positive contribution to B_2 and attractive interactions a negative one. Let us take the hard sphere potential as a typical example,

$$B_2(T) = -2\pi[\int_0^\sigma [\exp(-\infty) - 1] r^2 dr + \int_\sigma^\infty [\exp(0) - 1] r^2 dr] = 2\pi \int_0^\sigma r^2 dr \tag{64}$$

The last integration is easy to carry out and we obtain $B_2 = \frac{2\pi\sigma^3}{3}$. It is straightforward although somewhat lengthy to calculate the third and fourth virial coefficients as well and they are:

$$B_3 = \frac{5}{8} B_2^2 \tag{65}$$

$$B_4 = [-\frac{89}{280} + \frac{219\sqrt{2}}{2240\pi} + \frac{4131}{2240\pi} \arccos(\frac{1}{\sqrt{3}})] B_2^3 \tag{66}$$

Note that $B_2(T)$ is normally temperature dependent, the pure hard sphere potential is an exception, and this has the consequence that at a given temperature, *the Boyle temperature*, there is a perfect balance of attractive and repulsive interactions leading to $B_2(T_B) = 0$. This can be seen with a more realistic potential containing both attractive and repulsive interactions where B_2 can take both positive and negative values. As an example consider a gas interacting with a Lennard-Jones potential. There is of course not any analytical solution to the equation,

$$B_2(T) = -2\pi \int_0^\infty [\exp(-\beta 4\epsilon((\frac{\sigma}{r})^{12} - (\frac{\sigma}{r})^6) - 1] r^2 dr \tag{67}$$

but it can easily be solved numerically. Before doing so, it is convenient to make the variable substitutions $x = r/\sigma$ and $\xi = 4\beta\epsilon$, which give the more simple expression,

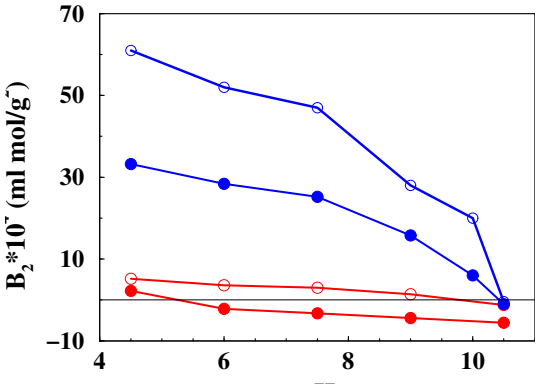

Figure 22: Measured (filled symbols) and simulated (open symbols) second virial coefficients, B_2, for lysozyme as a function of pH at two different NaCl concentrations - blue=100 and red=5 mM.

$$\frac{B_2(T)}{2\pi\sigma^3} = B_2^*(\xi) = -\int_0^\infty [\exp(-\xi(\frac{1}{x})^{12} - (\frac{1}{x})^6) - 1]x^2 dx \tag{68}$$

The dimensionless second virial coefficient B_2^* only depends on the parameter ξ. Hence, we may tabulate $B_2^*(\xi)$. Fig.(21) shows one curve from which we can calculate the coefficient for the whole range of parameter values.

The virial equation can also be applied to the interaction between solutes and one can define an *effective* second virial coefficient (cf. the Θ-temperature of polymer solutions). For example, the effective second virial coefficient of a dilute protein solution can be calculated from light scattering data. If there is an effective attraction between two protein molecules it will show up as an increased scattering in the experiment. One can also calculate $B_2^{eff}(T)$ for protein solutions using approximation which we will describe later. Fig.(22) shows how the virial coefficient varies in a lysozyme solution. At low pH values the protein has a large positive net charge giving a strong repulsive interaction, while at increasing pH and reduced net charge attractive van der Waals interactions start to dominate and B_2 approaches negative values.

3.5 Water as a dielectricum

Although the direct interaction of two ions in water is very strong it will be attenuated by the water molecules, so that the effective interaction is much weaker - this phenomenon is usually referred to as *dielectric* screening. This is a property of the solvent and is the same for all charged species. Typically dipolar liquids screen ionic interactions much better than apolar solvents. As a consequence, water has a very high dielectric constant, ϵ_r, and the effective interaction of two ions in water is reduced by ϵ_r,

$$w(r) = \frac{q_i q_j e^2}{4\pi\epsilon_0\epsilon_r r} \tag{69}$$

Eq.(69) is in principle only valid at infinite dilution. Extensive use of eq.(69) has, however, shown that it is an good approximation also at finite ion concentrations. Thus, one can with good confidence model water as a dielectric continuum and focus on ionic interactions. The approach is usually called *the primitive model* and has for many years been a cornerstone in electrolyte theory as well as in electric double layer theory. It appears in

Surfactant	CMC (mM)
$C_{12}SO_4^-Na^+$	8
$C_{12}SO_4^-Li^+$	9
$C_{12}SO_4^-K^+$	8
$C_{12}SO_4^-N(CH_3)_4^+$	6
$C_{12}SO_4^-N(Et)_4^+$	5

Table 1: The critical micelle concentration (CMC) for dodecyl sulfate chains with different counterions. The small variation in CMC is a consequence of the long range character of the Coulomb interaction.

Substance	ϵ_r	μ (D)	α ($4\pi\epsilon_0$ Å^3)	μ_A^2/v_A
Methyl formamide	182.4	3.9		0.18
Formamide	109.5	3.7		0.21
Water	78	1.85	1.5	0.11
Ethylene glycol	40.7	1.9		0.039
Methanol	32.6	1.7	3.2	0.043
Ethanol	24.3	1.7	5.2	0.030
Chlorobenzene	5.8	1.8		0.019
Benzene	2.3	0.0	10.6	
Hexane	2.0			

Table 2: Properies of different solvents: dielectric permittivity (ϵ_r), dipole moment (μ) and polarizability (α). The dielectric permittivity is given for room temperature. 1 Debye(D) = 3.36 10^{-30} Cm.

the context of colloid stability and polyelectrolyte solutions to name a few examples. One manifestation of the long range properties of ionic interactions is the relative insensitivity of the critical micelle concentration (CMC) of ionic amphiphiles to the type of counterion. For example, changing counterion from a sodium to a tetraethylammonium ion has only a marginal effect on CMC - see Table 1.

The dielectric permittivity can vary quite a lot for different solvent and Table 2 contains ϵ_r for a few representative solvents. A high dipole moment usually leads to a high dielectric constant, but the size of the molecule is also important. When trying to estimate the dielectric constant for a solvent, the dipole moment per volume, μ_A^2/v_A, is a good guide, (v_A is the molecular volume.)

The dielectrically screened Coulomb potential, eq.(69), is an effective potential, that is we have averaged the ion-ion interaction over the water coordinates. Formally one can write it as,

$$w(r) = \frac{q_i q_j e^2}{4\pi\epsilon_0\epsilon_r r} \approx -kT \ln \int d\mathbf{R}^N \exp[-\beta u(r, \mathbf{R}^N)] \tag{70}$$

where $\mathbf{R}^N$ denotes the coordinates for all water molecules and r is the ion-ion separation. This means that one measures the interaction between a pair of ions in a solution and average over all possible conformations of the solvent and the effect of the solvent becomes incorporated into ϵ_r. The resulting force between the two ions is not a mechanical force, but a thermodynamic force, *i.e.* it will depend on temperature and density. This has some intriguing effects. Let us apply eq.(52) $w(r)$ in eq.(69),

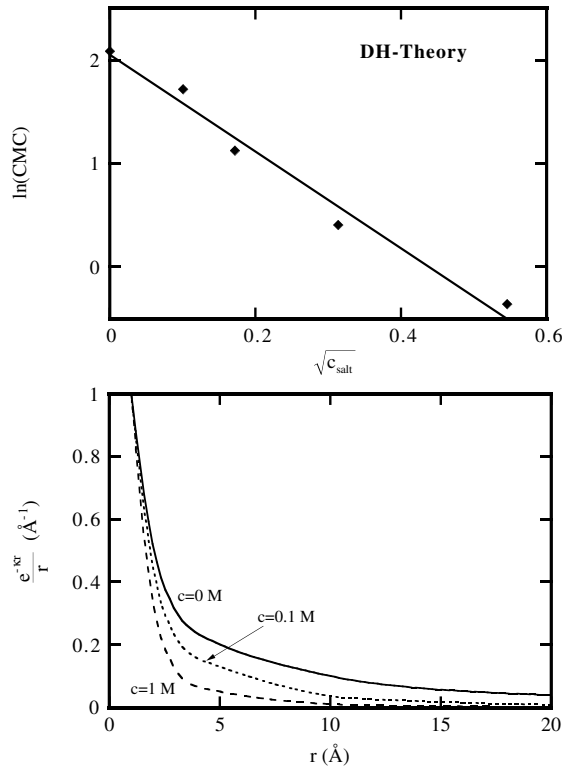

Figure 23: a) The variation of CMC with salinity. The straight line is a fit to the experimental data points. Debye-Hückel theory predicts a linear relation between ln(CMC) and salt concentration, as seen below from eq.(78). b) The decay of the electrostatic potential at three different salt concentrations.

$$< U(r) >= \frac{\partial \beta w}{\partial \beta} = w + \beta \frac{\partial w}{\partial \beta} = \frac{q_i q_j e^2}{4\pi\epsilon_0 \epsilon_r r}(1 + \frac{\partial \ln \epsilon_r}{\partial \ln T}) \tag{71}$$

The derivative $\frac{\partial \ln \epsilon_r}{\partial \ln T}$ is negative for most dipolar liquids and for water at room temperature it is about -1.36. This means that the sign of $< U(r) >$ is opposite to that of $w(r)$! Hence, the free energy of interaction between two oppositely charged ions in water is attractive, but the energy of interaction is repulsive.

3.6 Screened Coulomb interaction

Solutions containing charged species, which could be small atomic ions or highly charged aggregates, have special physico-chemical properties. This is due to the long range nature of the Coulomb potential decaying as r^{-1}. Already small concentrations of an electrolyte ($\approx$1 mM) will lead to markedly non-ideal behaviour. Addition of inert salt causes large changes in colloidal stabilities, reaction rates and titration curves. Electrolytes of various kinds have a profound influence on surfactants and polymers in solution. For example, in a solution containing ionic surfactants, the addition of inert electrolyte will significantly lower the CMC as is demonstrated in Figure 23a. Thus, electrostatic effects in solution are important and fortunately they can be qualitatively and sometimes quantitatively understood from simple Debye-Hückel (DH) theory.

The electrostatic potential ϕ is related to the charge distribution ρ via Poisson's equation

$$\epsilon_r \epsilon_0 \Delta\phi(x,y,z) = -\rho(x,y,z) \tag{72}$$

where Δ is the Laplace operator ($\frac{\partial^2}{\partial x^2} + \frac{\partial^2}{\partial y^2} + \frac{\partial^2}{\partial z^2}$). The problem is simplified by assuming spherical symmetry, in which case the Laplace operator becomes,

$$\Delta = \frac{1}{r}\frac{\partial^2 (r\phi)}{\partial r^2} \tag{73}$$

In order to proceed one has to find an expression for the charge distribution, that is how the ions distribute themselves in the electrostatic potential. By assuming that the ions are distributed according to Boltzmann's distribution law,

$$\rho(r) = Zec_0 \exp[-\frac{Ze\phi(r)}{k_B T}] \tag{74}$$

around the central ion positioned at the origin we arrive at the so-called Poisson-Boltzmann (PB) equation,

$$\epsilon_r \epsilon_0 \Delta\phi(r) = -\sum_i Z_i e c_{i0} \exp[-\frac{Z_i e\phi(r)}{k_B T}] \tag{75}$$

where Z_i is the ion valency, k_B is Boltzmann's constant, T the temperature and c_{i0} the ionic concentration at infinity. This is a non-linear equation and usually difficult to solve, but by linearizing the exponential ($e^x = 1+x+x^2/2+\ldots$) one obtains a tractable equation,

$$\Delta\phi(r) = \kappa^2\phi(r) \qquad \kappa^2 = \frac{\sum_i c_{0i} Z_i^2 e^2}{\epsilon_r \epsilon_0 kT} \tag{76}$$

where the Debye-Hückel screening length, κ^{-1} has been introduced. The final expression for the potential is given by,

$$\phi(r) = \frac{Ze}{4\pi\epsilon_r\epsilon_0(1+\kappa R)}\frac{\exp[\kappa(R-r)]}{r} \tag{77}$$

where R is the ionic radius. This is a simple yet very important result. It shows that the potential around an ion in a salt solution does not decay as $1/r$ but as $\exp(-\kappa r)/r$. This means that the electrostatic interaction has a much shorter range, depending on κ^{-1}, which in turn depends on salt concentration and valency - see Figure 23b. The physical interpretation is that the central ion attracts oppositely and repels equally charged ions, thereby creating the screening. Another important equation is obtained for the excess chemical potential, which in the DH theory reads,

$$\mu_{ex} = kT\ln\gamma = -\frac{\kappa Z^2 e^2}{8\pi\epsilon_0\epsilon_r(1+2R\kappa)} \tag{78}$$

where we also have defined the activity factor, γ. Eq.(78) can be reformulated with the aid of the *Bjerrum length*, $l_B = e^2/4\pi\epsilon_0\epsilon_r kT$ for a dilute 1:1 salt solution.

$$\ln\gamma \approx -\frac{\kappa l_B}{2} \tag{79}$$

For water at room temperature one finds that l_B =7.14 Å. This means that one can expect significant departure from ideal behaviour of an electrolyte solution when $\kappa^{-1} < l_B$. Note

Salt	κ^{-1} (Å)
1 M NaCl	3
10 mM NaCl	30
100 μM NaCl	300
1mM NaCl	95
1 mM $CaCl_2$	39
1 mM $AlCl_3$	27

Table 3: The screening length for some simple salts in aqueous solution and at room temperature.

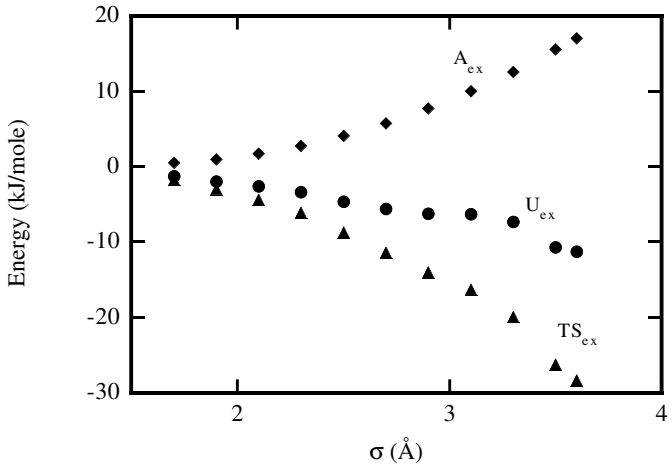

Figure 24: Monte Carlo simulations of the hydrophobic effect: a) The free energy of hydration for a Lennard-Jones particle in water. The ϵ-parameter is kept constant equal to 0.62 kJ/mol, while the σ-parameter is varied. The energy and entropy contributions are shown separately ($A_{ex} = U_{ex} - TS_{ex}$).

that $\kappa^{-1} = l_B$ corresponds to a concentration of about 175 mM. The screening length is an essential parameter for both qualitative and quantitative discussions. Fromeq.(77) it can be seen that the role of electrostatic interactions is reduced at separations $> \kappa^{-1}$. For an aqueous 1:1 salt solution at room temperature the screening length is 3 Å Since it is inversely proportional to c, one finds that $\kappa^{-1} = 30$ Å in a 10 mM salt solution. The valency also plays a role and high valency salts are very efficient in screening electrostatic interactions - see Table 3. A word of caution; the DH theory works excellently for 1:1 salts in aqueous solution, but it strongly underestimates the screening of charged aggregates in the presence of oppositely charged multivalent (counter)ions.

3.7 Hydrophobic interaction

The force responsible for the aggregate formation has to be found somewhere else. We have previously seen that the water-water interaction is comparably strong due to the hydrogen bonds formed between water molecules. Hence, introducing a non-polar molecule into water strongly disturbs the hydrogen bond network with a loss of interaction energy. The loss can be minimized if the water molecules around the solute adjust themselves, but the price has to be paid in lowered entropy. As a consequence, one usually finds that the free energy of transfer of a non-polar molecule into water at room temperature contains a large entropy contribution - see Figure 24. When dissolving non-polar molecules (*e.g.* the hydrocarbon tails of surfactant molecules) they will try to minimize the damage to

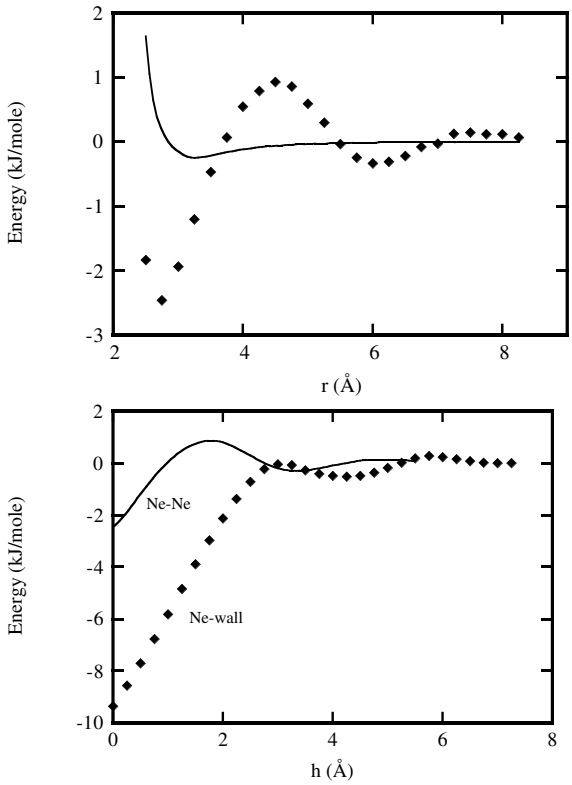

Figure 25: Monte Carlo simulations of the hydrophobic effect: a) The free energy of interaction between two neon atoms in liquid water. The solid line represents the interaction of two neon atoms in the gas phase. r is the distance between the two neon atoms. b) The free energy of interaction of a neon atom with a hydrophobic wall in liquid water (symbols) - the solid line shows the interaction of two neon atoms in liquid water. h is the separation between the wall and the center of mass of the neon atom. The solid curve is the same as the oscillating curve in a) with the minimum transfered to $h = 0$.

the water hydrogen bond network by aggregating. Figure 25a demonstrates the attractive interaction between two neon atoms in water. It is clear that this attraction is a solvation effect, *i.e.* the neon atoms are pushed together by the solvent (water). The corresponding interaction between two neon atoms in the gas phase has a much weaker attractive minimum. Figure 25b shows that replacing one of the neon atoms with an infinite hydrophobic wall, not unexpectedly, increases the attraction further. The hydrophobic interaction is the mechanism that promotes the formation of micelles. Table 4 shows that the longer the hydrocarbon tail a surfactant molecule carries, the more easily it will aggregate as indicated by the lowered CMC.

The hydrophobic interaction can be of considerable strength and is a delicate balance of energetic(enthalpic) and entropic terms. It is now also generally accepted to be the

Surfactant	CMC (mM)
$C_8SO_4^-$	160
$C_{10}SO_4^-$	40
$C_{12}SO_4^-$	10
$C_{14}SO_4^-$	2.5

Table 4: The critical micelle concentration (CMC) for alkyl sulphate chains with different chain length. The decrease in CMC is a consequence of the hydrophobic interaction between the alkyl chains.

main driving force for protein folding. Different arguments can be pursued in favour of one or another explanation of this interaction. One way though to understand it is by realizing the strong cohesive energy in the water-water interaction. The interaction is further emphasized by the orientational dependence, and any attempt break the structure will cost free energy; whether it appears in the form of an entropy or energy term is secondary. For apolar molecules like hydrocarbon this free energy loss can not be regained through interaction with the solute.

One simple estimate of the free energy cost of transferring a hydrocarbon molecule from its non-polar environment to water, is given by,

$$G_{transfer} = \gamma 4\pi R^2 \tag{80}$$

where γ is the interfacial tension and R the solute radius ($\gamma = 0.05$ J/m^2). The same type of expression can also be used to estimate the hydrophobic interaction between two non-polar solutes at contact,

$$G_{contact} = -\frac{\gamma 4\pi R^2 r}{R+r} \approx -\gamma 4\pi R r \tag{81}$$

where r is the radius of a water molecule. Eq.(81) is obtained by calculating the area inaccessible to water molecules. This can be done from simple geometry by considering two solute spheres in contact with a sphere representing a water molecule.

A semiquantitative measure of the solvent ability to dissolve non-polar molecules is given by the so-called Gordon parameter $= \gamma/V^{1/3}$ (J/m^3), where γ is the surface tension of the solvent and V its molar volume. Water has a very high Gordon parameter, ≈2.7, while hexane has a very low value of ≈0.3 (see Figure 26). Thus, we see that the hydrophobic interaction is largely due to the high cohesive energy density in water. One can also note that water is actually a "better solvent" than its high Gordon parameter implies, which means that water to some extent is capable of compensating for the loss in cohesive energy when dissolving a non-polar solute. (The four data points for water do not fit into the linear relationship). Thus, we have a clear qualitative understanding of the hydrophobic interaction in surfactant assemblies but lack a quantitative description of it. This is in contrast to the effective potential between two ions in solution, where eq.(69) provides an accurate representation of the interaction.

3.8 Potential of mean force

From what have been said above it is quite clear that even if all coordinates specifying a system are defined, it is not possible to define an interaction energy between two molecules in a solvent. It is however possible to define an effective interaction between two molecules in a similar way as was done in gas phase. To illustrate this we will start by considering two argon atoms in water. We will denote the relevant argon-argon distance by r and use R to specify all other coordinates. With this notation we can write the configurational integral,

$$Q = \int_r \int_R exp(-\beta E(r,R)) dr dR = \int_r q(r) dr \tag{82}$$

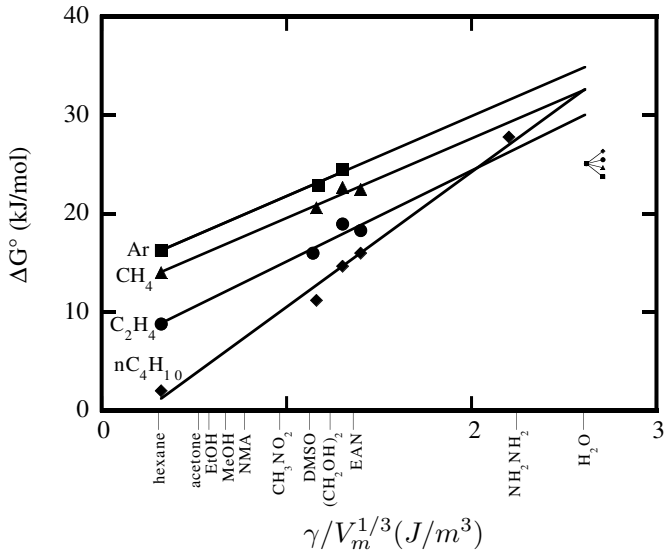

Figure 26: The free energy of transfer of a non-polar gas molecule into different solvents as a function of its Gordon parameter. The energy increases approximately linearly with the Gordon parameter for most liquids. Water on the other hand shows a significant deviation. (Redrawn from D. F. Evans and H. Wennerström, The colloidal domain, VCH, New York, 1994.)

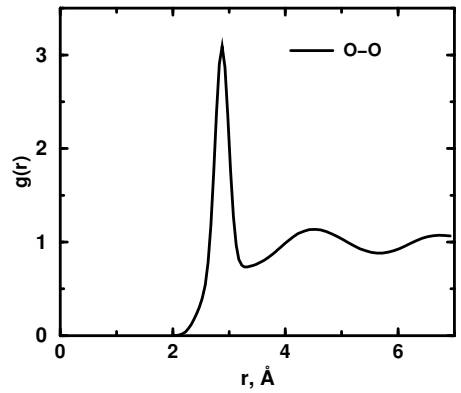

Figure 27: The radial distribution function for oxygens in liquid water at room temperature.

Thus, $q(r)$ is the contribution to the integral from configurations with an argon-argon distance r. The probability of a distance r can thus be obtained from,

$$P(r) = \frac{q(r)}{Q} \tag{83}$$

It is now straight forward to convert this probability into a free energy curve according to

$$w(r) = -kT[lnP(r) - lnP(\infty)] \tag{84}$$

where $w(r)$ is the potential of mean force between the two argon atoms. $P(r)$ is available from X-ray or neutron diffraction measurements. It can also easily be calculated from Monte Carlo or Molecular Dynamics simulations. It is straightforward to generalize this procedure for polyatomic systems. Experimentally one normally determines the probability of finding certain atoms separated by a given distance. In Figure 27 we show the probability of finding an oxygen atom at a specified distance from an other oxygen atom in water.

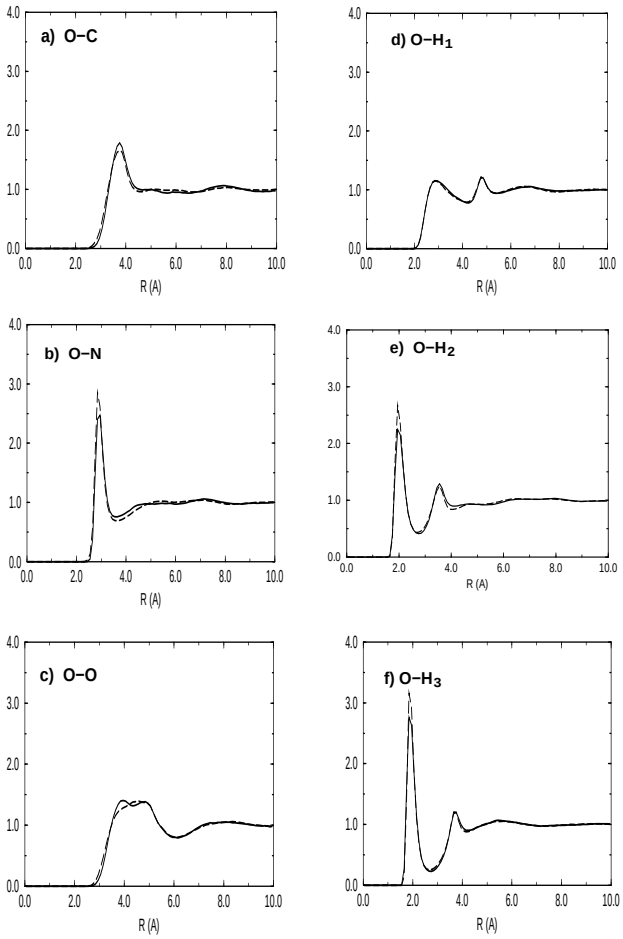

Figure 28: The radial distribution functions for different atom pairs in liquid formamide at room temperature.

The characteristic features are the oscillations in the probability. These oscillations are effects of the packing constraints in the system and are not directly related to the water

water pair potential. The oscillations look very much the same in all liquids. Another characteristic feature is that at larger distances the curve approaches unity, indicating that at long distances there is no effective interaction between two water molecules in water, or two argon atoms in argon. Finally we will ask the related questions: What is the potential of mean force between two argon atoms in water or between two water molecules in argon? In general terms the questions are easy to answer. The system will be dominated by the water - water interactions and the number of water - water contacts will be maximized. This means that on top of the oscillating contribution from the packing there will be an attractive long range interaction for both systems.

4 The Interaction of Macroscopic Bodies

Phase diagrams, coagulation kinetics, electrophoresis etc., give indirect information on the forces acting in a system. To directly measure the force between two macromolecules in a solution is more difficult. The osmotic stress technique is an excellent method for systems that spontaneously form, for example, lamellar structures. The system is in equilibrium with a bulk aqueous solution, whose chemical potential and osmotic pressure can be controlled. The aggregate spacing is measured by x-ray and at equilibrium the bulk osmotic pressure should be equal to the pressure acting between the aggregates.

The surface force apparatus (SFA) is technically more involved, but also more versatile. It consists of two crossed cylinders covered by smooth negatively charged mica sheets. the separation between the sheets can be measured interferometrically with a resolution of only a few Å. The force is measured by a set of springs and a piezoelectric crystal connected to one of the cylinders. The measured force between the curved cylinders can be converted to the free energy between planar surfaces using the Derjaguin approximation (see below). The SFA has an advantage in that the mica surfaces can be modified by adsorption and hence the interaction between, for example, polymer or protein covered surfaces can be measured. The atomic force microscope (AFM) and scanning tunnelling microscope are additional techniques that allow direct maesurement of forces between macromolecules and a larger aggregates.

The general rule, however, is that thermodynamic data is more reliable than different kinds of surface force measurements. This is so because of the risk for pollution - a macroscopic sample is not so easily polluted. The SFA or AFM are also rather delicate techniques and it is not difficult to get funny results.

4.1 The interaction of a molecule and a surface

Let us henceforth assume that molecules interact via an attractive potential $u(r) = -C/r^n$. Assuming additive interactions we can then integrate up the total interaction as,

$$W_{pw}(D) = -C\rho \int_D^\infty dz \int_0^\infty dr \frac{2\pi r}{(r^2+z^2)^{n/2}} \tag{85}$$

It is a straigthforward integration and we obtain the final expression,

$$W_{pw}(D) = -\frac{2\pi C\rho}{(n-2)(n-3)} \frac{1}{D^{n-3}} = -\frac{\pi C\rho}{6D^3} \quad (n=6) \tag{86}$$

If the initial interaction is of dispersion type, then the final interaction will be proportional to D^{-3}, that is much longer ranged than the initial one.

4.2 The interaction of a sphere and a surface

We can now proceed and study the interaction of a sphere of finite radius R interacting with an infinite wall. D denotes the distance between the spherical surface and the wall. Let us cut circular slices from the sphere each of which with the volume $\pi(2R-z)zdz$,

$$W_{sw}(D) = -\frac{2\pi^2 C\rho^2}{(n-2)(n-3)} \int_{z=0}^{z=2R} dz \frac{(2R-z)z}{(D+z)^{n-3}} \tag{87}$$

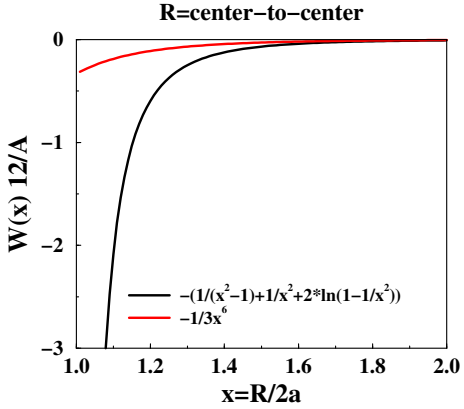

Figure 29: The van der Waals interaction between two spheres of radius a. The black curve shows the exact result, where the interaction have been integrated over the volumes of each of the spheres. The red curve displays the asymptotic $1/R^6$ result.

We can solve this integral exactly and the final expression can be simplified by noting that for $D \ll R$,

$$W_{sw}(D) = -\frac{4\pi^2 C\rho^2 R}{(n-2)(n-3)(n-4)(n-5)}\frac{1}{D^{n-5}} = -\frac{\pi^2 C\rho^2 R}{6D} \tag{88}$$

where the last equality holds for an r^{-6} interaction. These expressions can be used for some qualitative discussions. Consider, for example, the ratio between W_{sw}/W_{pw} with the denominator multiplied with the number of particles in the sphere.

$$\frac{W_{sw}}{W_{pw}} = \frac{\frac{\pi^2 C\rho^2 R}{6D}}{\frac{2\pi C\rho}{6(R+D)^3}4\pi R^3\rho/3} = \frac{3}{4}\frac{(R+D)^3}{DR^2} \approx \frac{R}{D} \tag{89}$$

Let us assume that a protein is 3 Å from a surface and that its radius is 20 Å. The ratio then becomes 7.6, which is approximately equal to the ratio $\frac{R}{D}$. Thus, we see that for large spheres close to surfaces we get a considerable contribution from geometrical factors (macroscopic).

4.3 The interaction of two spheres

The interaction of two spheres plays an important role in the theory of colloidal stability. Quite often the attractive part of this interaction comes from the van der Waals term. Consider, for example, the interaction of two proteins each with a radius of a. Since there is a dispersion attraction between all the atoms in protein 1 with all the atoms in protein 2, we have to sum up, or integrate, all the $1/r^6$ interactions. Doing this we obtain the expression,

$$W(R) = -\frac{A}{6}[\frac{2a^2}{R^2-4a^2} + \frac{2a^2}{R^2} + \ln(\frac{R^2-4a^2}{R^2})] \tag{90}$$

where R is the center-to-center separation and a is the protein radius. The expression can be written in a more transparent way if we introduce the variable $x = R/2a$

$$W(R) = -\frac{A}{12}[\frac{1}{x^2-1} + \frac{1}{x^2} + 2\ln\frac{x^2-1}{x^2}] \tag{91}$$

It is interesting to compare eq.(91) with $-C/r^6$ term acting between two atoms whose separation, R, is larger than their molecular dimensions, a. The coefficient C should of course be multiplied with N^2, where N is the number of atoms in a protein. The resulting expression can be written as,

$$W_{approx}(R) = -\frac{A}{36}\frac{1}{x^6} \tag{92}$$

Fig.29 shows a comparison between the results from eqs.(91) and (92). Obviously, the simple $-1/R^6$ is not applicable at short separation, since it gives a completely different separation dependence.

4.4 The interaction of two surfaces

We can proceed to calculate the interaction of two surfaces, but it has to be done per surface area otherwise the result will diverge. Hence we write,

$$W_{ww}(D) = -\frac{2\pi C\rho^2}{(n-2)(n-3)}\int_{z=D}^{z=\infty}\frac{dz}{z^{n-3}} \tag{93}$$

which is

$$W_{ww}(D) = -\frac{2\pi C\rho^2}{(n-2)(n-3)(n-4)}\frac{1}{D^{n-4}} = -\frac{\pi C\rho^2}{12D^2} \tag{94}$$

where the last equality holds for an r^{-6} interaction.

4.4.1 "Johanssons passbitar"

A famous Swedish invention was finely polished metal pieces, which were used for precision measurements in industrial workshops. The precision was very high, 10^{-6} m, and the polished metal surfaces adhere very strongly. Why do the metal pieces stick together? Let us consider a simple example: From eq.(94) we know that the pressure is $P_{ww} = -\frac{\pi C\rho^2}{6D^3}$ and the coefficient is roughly $4\cdot 10^{-20}$, the contact area is 10^{-4} m^2. With a separation of:

- $D = 1000$ Å we get $F = 4$ mN
- $D = 100$ Å we get $F = 4$ N
- $D = 10$ Å we get $F = 4000$ N

4.5 The Derjaguin approximation

The force between two surfaces, curved or not is simply $F(D) = -\partial W(D)/\partial D$. From inspection of eqs.(88) and (94) for W_{sw} and W_{ww} one finds that,

$$F_{sw}(D) = 2\pi R W_{ww}(D) \tag{95}$$

This is a result of a more general relation between curved and planar surfaces called *the Derjaguin approximation*. To see this, consider the interaction of two spheres with radii R_1 and r_2 whose surface-surface interaction can be described by $f(Z)$ (per unit area).

$$F(D) = 2\pi\int_{Z=D}^{Z=2(R_1+R_2)} dx\, x f(Z) \tag{96}$$

where x can be calculated from the chord theorem as $Z = D + (x^2/2)(1/R_1 + 1/R_2)$ and the derivative is then easily found as $dZ = (1/R_1 + 1/R_2)x\,dx$. Let us replace the upper limit with ∞ and we obtain,

$$F(D) = 2\pi \frac{R_1 R_2}{R_1 + R_2} \int_{Z=D}^{Z=\infty} f(Z) dZ = 2\pi \frac{R_1 R_2}{R_1 + R_2} W(D) \tag{97}$$

5 Electrostatic Forces

Colloidal particles, biopolymers and membranes all carry charges in an aqueous environment. The molecular source of these charges can be covalently bound ionic groups like phosphates, sulfates, carboxylates, quartenary ammoniums or protonated amines. The carboxylates and amines can titrate in response to pH changes, while the other groups remain charged except at extreme conditions. A particle, a self assembled aggregate or a polymer can also acquire a charge by adsorption of a small charged molecule like an amphiphile. The interactions between charged mesoscopic objects is strongly influenced by the net charge and the electrostatic interactions provide one of the basic organizing principles in both colloidal sols and in living cells. These electrostatic interactions can be both attractive, leading to association, and repulsive resulting in dispersion. The technical/commercial importance of charged surfaces and how to control their properties is immense - Fig.30 gives one common example.

The basic description of electrostatic interactions between colloidal particles was worked out during the 1940's independently by Derjaguin and Landau in the Sovjet Union and by Verwey and Overbeek in the Netherlands. Both groups based their description of the electrostatic effects on the Poisson-Boltzmann (PB) equation, as in the Gouy-Chapman theory of a single charged surface, and the Debye-Hückel theory of electrolyte solutions. Combined with a description of van der Waals interactions, the resulting DLVO theory has played an immense role for our understanding and description of interactions in colloidal systems.

As all theories the DLVO approach has its limitations coming from both the model and approximations. The theory is based on a continuum description of two media separated by a sharp interface. All real interfaces have a finite width and the DLVO theory can be expected to work properly only at separations that exceed this width. For smooth liquid-solid interfaces, *e.g.* mica-water, this is not a severe limitation, while for surfaces with adsorbed polymers the DLVO contribution to the interaction can become irrelevant. Similarly, one can at interfaces often have lateral correlations, or inhomogeneities, causing deviations from the continuum description for perpendicular separations of the order of the lateral correlation length. Another, more subtle, source of a breakdown of the DLVO description is the mean field approximation inherent in the Poisson-Boltzmann equation. Before entering into the electrostatic interactions let us consider a simple ideal gas and ask wherefrom the forces in the system come.

5.1 The ideal gas

The total force in a macroscopic system contains both an energy and an entropy term. It is easy to find systems where the force is dominated by the entropy derivative. The ideal gas is one and an ordinary rubber band is another. We find the force (or pressure) from the derivative of the free energy, $A = E - TS$,

$$Force = -\frac{\partial A}{\partial R} = -\frac{\partial E}{\partial R} + T\frac{\partial S}{\partial R} \tag{98}$$

Let us study the ideal gas, for which we can easily write up the total partition function,

Figure 30: Diapers are good examples of charged surfaces and the force originating from counterion entropy.

$$Q_N = \frac{1}{h^{3N}N!}(2\pi mkT)^{3N/2}V^N \tag{99}$$

We know that the free energy is equal to , $A = -kT\ln Q_N$, from which follows that

$$p = -\frac{\partial A}{\partial V} = \frac{\partial \ln Q_N}{\partial V} = kT\frac{\partial \ln V^N}{\partial V} = \frac{NkT}{V} \tag{100}$$

This is the ideal gas law. Let us now take one step backward and partition the free energy into its energy and entropy components, respectively. If the gas is monoatomic, which we can assume for simplicity, then the energy is just the translational energy, $E = \frac{3}{2}kT$ and the entropy is, $-TS = A - E$. Now take the derivative of these two terms separately in order to distinguish the two pressure component, p_E and p_S.

$$p_E = -\frac{\partial E}{\partial V} = 0 \qquad p_S = T\frac{\partial S}{\partial V} = \frac{NkT}{V} \tag{101}$$

Note that the entropy can be written as,

$$S = k\ln[\frac{1}{h^{3N}N!}(2\pi mkT/e)^{3N/2}V^N] \tag{102}$$

Thus, the pressure is a pure entropic term!

The partition function, eq.(99), consists of three different terms:

- $\frac{1}{h^{3N}N!}$ which is a quantum correction.
- $[\frac{(2\pi mkT)^{3/2}}{h^3}]^N$ comes from the integration over the momenta.
- V^N which comes from an integration over the spatial coordinates

This is an indication that one should be careful when discussing forces as a result of kinetic effects. In classical statistical mechanics kinetics NEVER enters into equilibrium properties.

5.2 Charged surfaces

How does a charged surface appear and where do the charges come from? The fact is, that most products contain charged surfaces, *e.g.* food, dipers, paints, etc. Let us give a few examples:

- Titrating groups, that is the charge will vary with pH, *e.g.* polyacrylic acid.

$$RCOOH \rightarrow RCOO^- + H^+$$

- Adsorption of ions onto a solid surface, *e.g.* AgI(s).

$$AgI(s) + I^- \rightarrow AgI^-(s) \qquad AgI(s) + Ag^+ \rightarrow AgI^+(s)$$

- Dissociation of a salt or mineral. Glass is a good example.

$$R - O^- Na^+(s) \rightarrow R - O^-(s) + Na^+$$

- Proteins, several amino acids are charged at neutral pH, *e.g.* glutamic acid, lysine etc.
- Biological membranes often contain 10-20 per cent of charged lipids, phosphatidyl choline is zwitterionic, while phosphatidyl serine is negatively charged.

$$[CH_3 - (CH_2)_n - CH_2]_2 - OPO_3^- - CH_2 - CH_2 - N^+ - (CH_3)_3 \qquad choline$$

$$[CH_3 - (CH_2)_n - CH_2]_2 - OPO_3^- - CH_2 - CH - N^+ - COO^- \qquad serine$$

- Micelles and other soap aggregates.

The geometry can vary quite a lot, but the systems retain a lot of common characteristics. Idealized geometries are often plane, sphere or cylinder. The technical applications are very profound, but we can still approach the problem on a rather sophisticated theoretical level. Let us do that and in the following we will initially restrict the treatment to two planar charged surfaces with only neutralizing counterions in between.

5.3 Salt-free double layer

We have seen above that the geometry of charged aggegates can vary a lot, but they still have a number of properties in common. With this in mind we can choose to study a planar geometry for mathematical convenience without loosing the important physical aspects. The typical model system is two infinite planar uniformly charged surfaces, but we can also in some cases limit the study to a single charged surface - see Fig.31. The questions we want to ask: How are the counterions distributed and how does the force

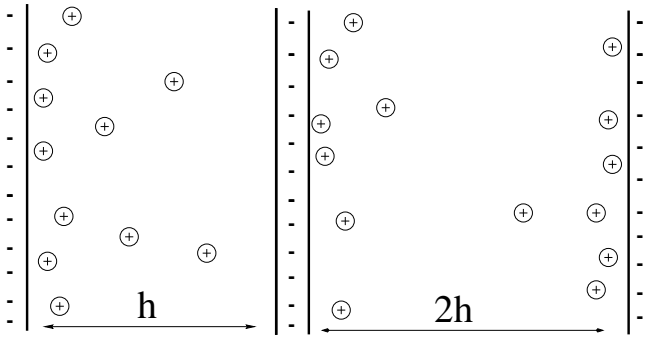

Figure 31: a) Schematic representation of a single charge wall and its counterions. b) Same as in a), but with two charge surfaces. Additional salt pairs have been left out for clarity.

vary with plane-plane separation? We will assume a dielectric continuum model and try to solve the appropriate equations. Let us start by introducing the potential, $\Phi(\mathbf{r})$ and the charge distribution, $\rho(\mathbf{r})$ in the Poisson equation,

$$\epsilon_r \epsilon_0 \Delta\Phi(\mathbf{r}) = -\rho(\mathbf{r}) \tag{103}$$

and combine this equation with the Boltzmann distribution,

$$\rho(\mathbf{r}) = \sum_i c_i Z_i e \exp[-Z_i e\Phi(\mathbf{r})/k_B T] \tag{104}$$

Let us now introduce cylindrical symmetry and write the combination as,

$$\frac{d^2\Phi(x)}{dx^2} = -\frac{cZe}{\epsilon_r \epsilon_0} \exp[-Ze\Phi(x)/k_B T] \tag{105}$$

This is an ordinary differential equation, but it does not have constant coefficients, hence it is in general very difficult to solve. But for the particular symmetry we have chosen, it has a solution and by using a trick,

$$\frac{d}{dx}(\frac{d\Phi}{dx})^2 = 2\frac{d^2\Phi}{dx^2}\frac{d\Phi}{dx} \tag{106}$$

which leads to the very nice and compact solution,

$$\Phi(x) = -\frac{2kT}{Ze}\ln[\cos(sx/h)] \qquad\qquad \Phi''(x) = -\frac{2kTs^2}{Zeh^2}\frac{1}{\cos^2(sx/h)} \tag{107}$$

where $2h$ is the plate separation and the parameter s is determined by the transcendental equation,

$$s\tan s = \frac{\mid \sigma \mid Zeh}{2kT\epsilon_r\epsilon_0} = \frac{h}{\lambda_{GC}} \tag{108}$$

where λ_{GC} is the so-called *Gouy-Chapman length* defined as,

$$\lambda_{GC} = \frac{e}{2\pi Z\sigma l_B} \tag{109}$$

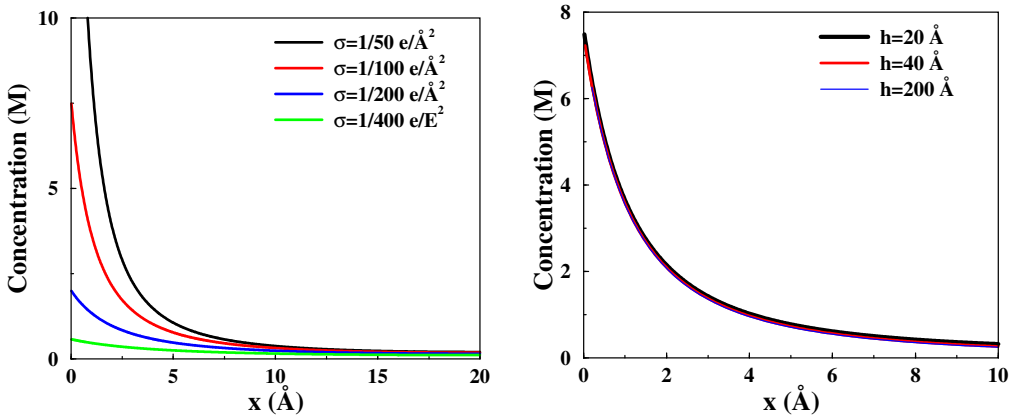

Figure 32: Counterion distribution outside a single charged surface as calculated from the Poisson-Boltzmann equation, eq.(110). Monovalent counterions, $\epsilon_r = 78.3$ and room temperature. a) Variation of surface charge density and b) variation of surface separation, $\sigma = 0.01$ e/Å^2.

5.3.1 Boundary concentrations

Let us see what the concentration or charge density are at the walls. The charge density is given by,

$$\rho(x) = -\epsilon_r\epsilon_0\Phi''(x) = \frac{2kTs^2\epsilon_r\epsilon_0}{Zeh^2}\frac{1}{\cos^2(sx/h)} \tag{110}$$

How the counterion concentration varies as a function of surface charge density can be seen from Fig.32. If we now introduce the two limits, we obtain,

$$\rho(h) = \frac{2kT\epsilon_r\epsilon_0}{Zeh^2}\frac{s^2}{\cos^2(s)} = \frac{\sigma^2 Ze}{2kT\epsilon_r\epsilon_0}\frac{1}{\sin^2(s)} \tag{111}$$

$$\rho(0) = \frac{2kTs^2\epsilon_r\epsilon_0}{Zeh^2} \tag{112}$$

What happens now if we dilute the system? That is we let $h \to \infty$. This means that the rhs. of eq.(108) becomes infinite and there is a trivial solution for $s = \pi/2$.

$$\rho(h) = \frac{\sigma^2 Ze}{2kT\epsilon_r\epsilon_0}\frac{1}{\sin^2(s)} = \frac{\sigma^2 Ze}{2kT\epsilon_r\epsilon_0} \qquad h \to \infty \tag{113}$$

$$\rho(0) = \frac{2kTs^2\epsilon_r\epsilon_0}{Zeh^2} = \frac{kT\pi^2\epsilon_r\epsilon_0}{2Zeh^2} \qquad h \to \infty \tag{114}$$

If we want to know the particle densities we have to divide by Ze. There are several interesting features in the above expressions. Firstly, we note that it is impossible to dilute away the counterions - *counterion condensation*. This is illustrated in Fig.110b for three different separations. Another feature is that the concentration at the midplane becomes independent of σ for large a. Note that we have chosen h as the variable here, but we could also have chosen some of the other parameters T, ϵ_r, Z or σ in order to approach the limit $s = \pi/2$.

5.3.2 Double layer repulsion

Now we proceed to forces or the pressure acting on the walls. Using the ordinary thermodynamic relation, $p \propto -\partial A/\partial h$, we can find the pressure by taking the derivative with

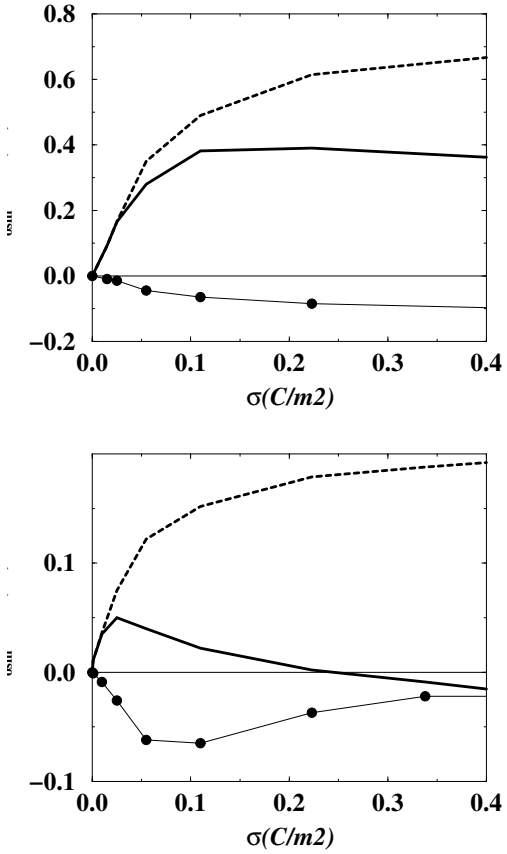

Figure 33: a) The osmotic pressure as a function of surface charge density for two planar double layers with neutralizing monovalent counterions separated a distance of 21 Å. The solid line is from Monte Carlo simulations and the dashed line from the PB equation. The thin line with symbols show the attractive contribution to the total pressure. b) The same as a) but with divalent counterions. Note the different scales in a) and b)!

respect to the midplane or to the charged wall. The result is

$$p_{osm} = kTc(h) - \frac{\sigma^2}{2\epsilon_r\epsilon_0} \qquad p_{osm} = kTc(0) + p^{corr} \tag{115}$$

These two relations are exact within the given modell (note that we have assumed point ions). The term p^{corr} comes from the fact that the ions on either side of the midplane correlate and it will give an attractive contribution to the pressure. Fig.33 shows how the osmotic pressure varies with surface charge density. Note that the pressure, as described in the mean field theory approch a limiting value. The pressure is also lower with divalent counterions, which seems reasonable from the simple fact that we only have half as many counterions. According to the PB equation, *cf.* eq.(114), the osmotic pressure varies approximately as $1/Z^2$. For $h \to \infty$ the pressure will go to zero, hence the first pressure relation gives us back one of the previous contact relations. If we now proceed by introducing a mean field approximation then the first pressure expression remains valid while in the second the approximation has by definition put $p^{corr} \equiv 0$. Thus, in the mean field we obtain a further relation,

$$c(h) - c(0) = \frac{\sigma^2}{2kT\epsilon_r\epsilon_0} \tag{116}$$

We can also write an explicite formulae for the osmotic pressure,

$$p_{osm} = \frac{2(kTs)^2\epsilon_r\epsilon_0}{(Zeh)^2} \tag{117}$$

The pressure at large separation decays like $1/h^2$, which is a rather funny dilution behaviour.

5.4 Cum granum salis

Qualitatively nothing happens when salt is added. Mathematically everything becomes much more complicated and there are only a few very special cases where it is possible to obtain a closed form solution. The contact relations for the pressure still holds after minor modifications,

$$p_{osm} = kT\sum_i c_i(h) - \frac{\sigma^2}{2\epsilon_r\epsilon_0} \qquad p_{osm} = kT\sum_i c_i(0) + p^{corr} \tag{118}$$

In the mean field the correlation term is still zero, but we have to include the pressure in the bulk in our calculations. This means that the net pressure now appears as,

$$p^{net}_{osm} = p^{dl} - p^{bulk} = kT\sum_i c_i(0) - kT\sum_i c_i^{bulk} \tag{119}$$

where we have used the mean field approximation also in the bulk.

We saw previously how counterions accumulate close to a charged surface, see Fig.32. The same accumulation is also seen when a surface is in contact with a salt reservoir containing both counterions and coions. In this case, the coions will be expelled from near the surface. Both the counterion and coion concentrations will approach a bulk value sufficiently far from the charged surface, which is demonstrated in Fig.34.

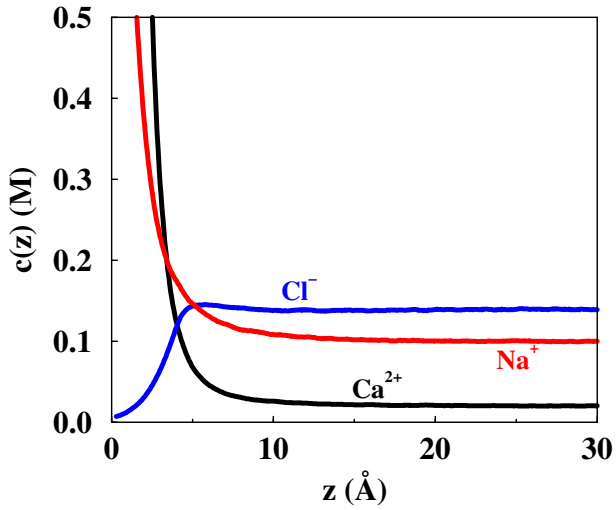

Figure 34: Counterion and coion distribution outside a charged surface as calculated from a Monte Carlo simulation. The bulk solution contains 100 mM of NaCl and 20 mM of $Ca(Cl)_2$.

In a more rigorous treatment we have to include also hard cores and the pressure in the bulk has to be calculated within an approximation of the same level, *i.e.* it does not make sense to perform a MC simulation for the double layer and use a mean field in the bulk. A more correct expression for the net pressure would be,

$$p_{osm}^{net} = kT \sum_i c_i(0) + p^{corr} + p^{coll} - p^{bulk} \tag{120}$$

Note that there must be an equilibrium between the bulk and double layer, that is $\mu_i^{dl} = \mu_i^{bulk}$.

5.4.1 Gouy-Chapman case

There is a special case with a single charged wall in contact with an infinite reservoir, where one can obtain a closed solution. Assuming that the reservoir consists of a 1:1 electrolyte, then we can reformulate the Boltzmann distribution, eq.(104),

$$\rho(x) = en_0[\exp(-e\Phi/kT) - \exp(e\Phi/kT)] = -2en_0 \sinh(e\Phi/kT) \tag{121}$$

n_0 is the bulk salt concentration. This can again be combined with the Poisson equation. The solution to the differential equation can be written as,

$$\Phi(x) = \frac{2kT}{e} \ln \frac{1 + \gamma \exp(-\kappa x)}{1 - \gamma \exp(-\kappa x)} \qquad \gamma = \frac{\exp(e\Phi_0/2kT) - 1}{\exp(e\Phi_0/2kT) + 1} \tag{122}$$

where $\Phi_0 = \Phi$(at the wall) and κ^{-1} is the Debye-Hückel screening length,

$$\kappa^2 = \frac{2e^2 n_0 z^2}{2\epsilon_r \epsilon_0 kT} = \frac{e^2 I}{2\epsilon_r \epsilon_0 kT} \tag{123}$$

Note the dependence of the screening length on $\sqrt{n_0}$ and on Z^2 (I = the ionic strength).

If the surface potential is low, then it is OK to make a series expansion of the exponential in eq.(122) and also of the logarithm in eq.(122). This allows us to write the potential,

$$\Phi(x) \approx \Phi_0 \exp(-\kappa x) \qquad \Phi_0 \approx \frac{\sigma}{\epsilon_r \epsilon_0 \kappa} \tag{124}$$

If two surfaces are far apart, then we can still apply the GC-solution (derived under the assumption of infinite separation). This procedure is usually refered to as the *weak overlap approximation* and it leads to a nice expression for the pressure between two surfaces in equilibrium with a bulk of salt concentration, n_0,

$$p_{osm}^{net} = 64kTn_0\gamma^2 \exp(-\kappa 2h) \tag{125}$$

The important thing here is the exponential decay. The experimental results are usually quite reliable with respect to this exponential decay, while the pre-factor is more shaky.

5.4.2 General solution

A general solution can only be obtained numerically or in formal terms of elliptic integrals. Note that the overlap expression predicts a rather strong valency dependence through κ. In the full non-linear treatment it is even larger and in MC simulation it becomes so strong that it also can revert the sign and lead to an attractive pressure, see below.

A charged surface may act as an ion exchanger - it prefers multivalent ions in favour of monovalent. Another interesting fact is that the chemical potential of the bulk and the double layer must be the same. This means that the salt concentrations are not the same! For purely entropic reasons it is difficult to get in more salt in the double layer, since it already harbours all the counterions.

- At small separations $h \ll \kappa^{-1}$we have,

$$\frac{n_{dl}}{n_0} \sim \frac{(\kappa h)^2}{2\pi^2} \tag{126}$$

  For a situation with $h = 25$ Å and $n_0 = 1$ mM, then the ratio is only 1/300.

- At large separations $h \gg \kappa^{-1}$we have,

$$\frac{n_{dl}}{n_0} \sim 1 - \frac{2}{\kappa h} \tag{127}$$

  This means that with 300 Å between the walls and 10 mM in the bulk there will be a 40 per cent deficit in the double layer.

5.4.3 The DLVO theory

The important use of the above mean field pressure is in combination with van der Waals forces into the so called *DLVO theory*. We have previously shown that the attractive vdW pressure decays algebraically like $1/h^3$. Thus, the total pressure can be written as,

$$p_{DLVO} \approx A \exp(-2\kappa h) - \frac{B}{a^3} \qquad \hat{p} = C \exp(-u) - \frac{1}{u^3} \tag{128}$$

where $u = 2\kappa h$ and the coefficient $C = A/8\kappa^3 B$. Figure 35 shows that increasing the salt concentration leads to a lower barrier. If the scale is expanded one may notice a second minimum, although very shallow.

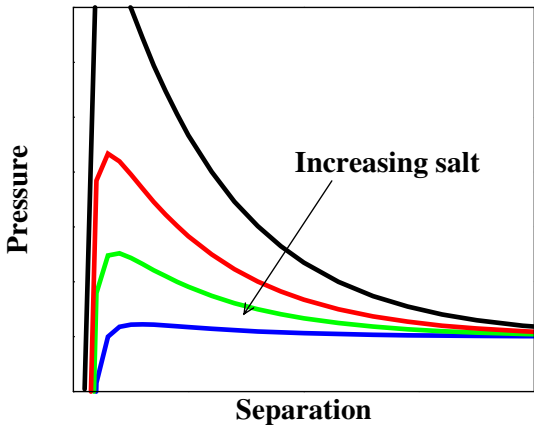

Figure 35: The DLVO potential for different salt concentrations. Plotted after the rescaled DLVO equation.

5.5 Beyond the mean field

- The ionic size gives a correction to the PB pressure and it is a repulsive correction.
- Discrete charges on the walls become important when $h \leq \sqrt{e/\sigma}$
- The dielectric continuum model will break down at short separations, when $h \approx R_{water}$

Another correction to the mean field is the correlation term in eq.(115). It can become important whenever the electrostatic coupling is large. One can show that the saltfree system is completely determined by two coupling parameters, S_1 and S_2, and that correlation effects become important when S_2 is large.

$$S_1 = \frac{4\pi\epsilon_0\epsilon_r kTh}{Z^2e^2} = \frac{h}{Z^2 l_B} \qquad S_2 = \frac{Z^3e^3\sigma}{(4\pi\epsilon_0\epsilon_r kT)^2} = \frac{Z^3 l_B^2\sigma}{e} \tag{129}$$

Hence we see that changing the valency or the dielectric permittivity has a significant effect on the correlation term. The former variation is illustrated in Fig.33b, where it is shown how the net osmotic pressure can become attractive for divalent counterions and high surface charge density. How can we understand this attraction and the appearance of the correlation term? The easiest example is the interaction of two spherical charge distributions.

5.5.1 Correlations between two spherical double layers

Let us first make clear that the derivation to follow is purely classical, but the use of statistical mechanical perturbation theory leads to an expression very similar to the one obtained for quantum mechanical dispersion forces. It is of course possible to perform a similar analysis in any geometry, but none will give as neat algebraic expressions as the spherical one. We also have a nice analogue in the dispersion term discussed at an early stage of these notes.
Consider two spherical cells, each of radius R_c and each containing one spherical macroion of charge Z_m and radius R_m. We will only consider saltfree cells, thus, each cell also

contains the necessary amount of neutralizing counterions. A distance R separates the macroion centers. The excess free energy due to the interaction of the two sub-systems can be written as,

$$\Delta A = kT \ln < \exp[-\Delta U(R)/kT] >_0 \tag{130}$$

$\Delta U(R)$ is the interaction energy between the cells for a particular configuration of counterions. The angular brackets $<>_0$ represent an average over the counterions in the individual non-interacting cells. The interaction energy $\Delta U(R)$, can be written as a two-center multipole expansion where the different terms represent charge-charge, charge-dipole, dipole-dipole interactions etc.,

$$\Delta U(R) = \int d\mathbf{r}_A d\mathbf{r}_B \frac{\rho_A(\mathbf{r}_A)\rho_B(\mathbf{r}_B)}{\mid \mathbf{r}_A - \mathbf{r}_B \mid} = \text{ion-ion} + \text{ion-dipole} + \text{dipole-dipole...} \tag{131}$$

It is obvious from symmetry considerations that the two first terms will disappear and that the first non-vanishing term is the dipole-dipole interaction. By expanding the logarithm and keeping only second order terms in the interaction and including the first non-zero term in the multipole expansion one obtains,

$$\beta \Delta A \approx -\frac{\beta^2}{2} < \Delta U^2(R) >_0 = -\frac{3\alpha_A \alpha_B}{R^6} \tag{132}$$

where α is a generalized polarizability for the counterions in their respective cells defined as,

$$\alpha = \frac{< (\sum_i zer_i)^2 >_0}{3kT 4\pi\epsilon_0\epsilon_r} \tag{133}$$

The analogy with the orientationally averaged dipole-dipole interaction, eq.(50) is immediate with a slightly different origin of the polarizabilities. Eq.(133) is also similar to the expression obtained for the quantum mechanical dispersion interaction, *cf.* eq.(29). The classical polarizabilities vary with aggregate charge and cell radius, but the difference between a system with monovalent or divalent counterions is small.

5.5.2 A simple double layer model

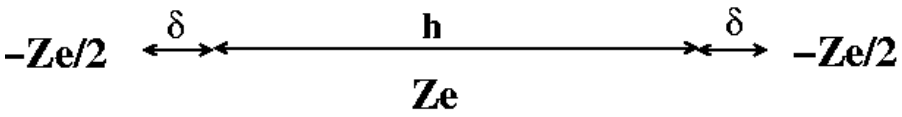

Figure 36: The simplified model with two fixed "surface" charges and one mobile counterion of valency Z confined to a line of length h. The displacement of the surface charges, δ, is supposed to mimick the surface charge density.

We can try to simplify the model in Fig. 31b one step further. If the interaction between the counterions is strong, then imagine a situation where each counterion is confined to its own little cylinder with the ends of the cylinder being the charged surfaces. That is, each cylinder contains only one counterion and we assume that there is no interaction between two cylinders. The extreme of this is of course if the counterion, of charge Ze,

only moves along the cylinder axis. In order to simplify the system further we also replace the charged circular surfaces with a point charge equal to $-Ze/2$ and finally we obtain the model system, depicted in Fig. 36. The distance δ is chosen such that the potential at the end points from the nearest surface is the same with a point charge as with a smeared out surface charge density on a circular area with radius R. That is, we have the condition,

$$\frac{(Ze/2)Ze}{4\pi\epsilon_0\epsilon_r\delta} = \int_0^R \frac{Ze\sigma 2\pi r dr}{4\pi\epsilon_0\epsilon_r r} \tag{134}$$

Noting that $\sigma = Ze/2\pi R^2$ we get,

$$\delta = \frac{R}{2} \qquad \text{and} \qquad \sigma = \frac{Ze}{8\pi\delta^2} \tag{135}$$

Thus, for a given counterion valency, the distance δ is a measure of the surface charge density. Let us now estimate the energy by placing the counterion in the middle between the "surfaces". The energy for that particular configuration is not as low as the average energy of the system. Likewise we can overestimate the entropy by assuming that the distribution is uniform. Using such a heuristic approach the free energy of the system can be written as,

$$A(h)/kT = -\frac{7Z^2 l_B}{4(h+2\delta)} - \ln\frac{h}{Z^2 l_B} = -\frac{7}{4(S_1 + 1/\sqrt{2\pi S_2})} - \ln S_1 \tag{136}$$

where we have used the dimensionless parameters introduced above. A constant, $kT\ln Z^2 l_B$, has also been added in order to make the entropic term dimensionally consistent. Note that the terms in eq.(136) depends in a qualitatively correct way on the same dimensionless parameters as those of the more elaborate model, Fig. 31. There is a competition between an entropic term that dominates for large S_1, *i.e.* large separations, and also for very small S_1, while the interaction term can dominate at intermediate separations provided that S_2 is sufficiently large. The force, F, acting on the fixed charges is determined by the derivative,

$$F = -\frac{\partial(A(h)/kT)}{\partial S_1} = -\frac{7}{4(S_1 + 1/\sqrt{2\pi S_2})^2} + \frac{1}{S_1} \tag{137}$$

By solving for the condition of $F = 0$ at a finite value of S_1 we obtain the requirement $S_2 \geq 128/49\pi$ for a non-monotonic variation of the force. For monovalent counterions in an aqueous system it is essentially impossible to reach a surface charge density so that S_2 exceeds the critical value $128/49\pi \approx 0.83$, while this is readily achieved for counterions of higher valency. As an explicit example choose $\sigma = 0.07$ C/m^2 ($\approx 1e/200$ Å^2), in an aqueous system at room temperature ($l_B = 7.1$ Å). For monovalent ions $S_2 = 0.22$, which is well below the critical value, while for divalent counterions we have $S_2 = 1.76$, which yields a force curve with a primary minimum. For $Z = 3$ $S_2 \approx 12$ and as shown in Fig. 37a this results in a strongly attractive force curve.

For room temperature and aqueous conditions, the limiting charge density for a non-monotonic force curve corresponds to:

- $\sigma = 0.26$ C/m^2, $h = 6.2$ Å, $Z = 1$
- $\sigma = 0.033$ C/m^2, $h = 25$ Å, $Z = 2$

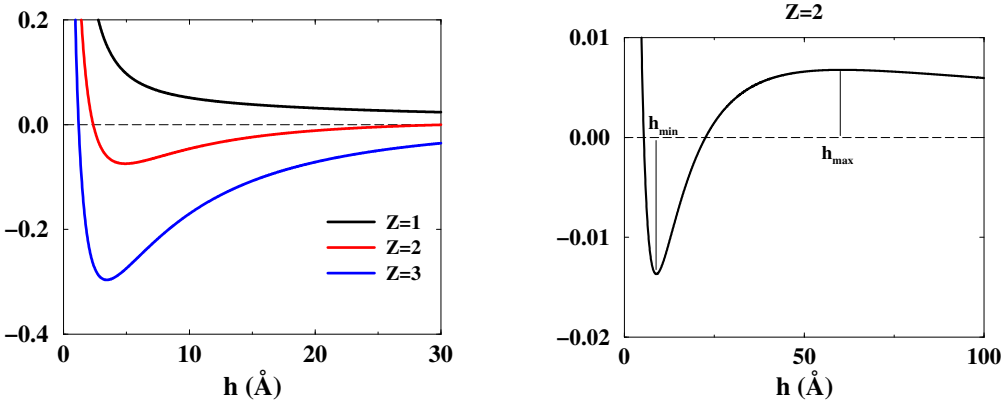

Figure 37: a) The force between the two fixed charges in the simplified "double layer". The counterion valency has been varied, while $\sigma = 0.07$ C/m^2. b) The van der Waals' loop in the force curve indicating a phase transition.

- $\sigma = 0.010$ C/m^2, $h = 55$ Å, $Z = 3$

When σ increases beyond these values, then the minimum in the interaction moves to shorter separations according to,

$$S_1 = \frac{7}{8} - \frac{1}{\sqrt{2\pi S_2}} \pm \sqrt{(\frac{7}{8})^2 - \frac{7}{4\sqrt{2\pi S_2}}} \tag{138}$$

The plus sign gives the position of the maximum of the force curve. At high surface charge densities, $S_2 \gg 1$, then eq.(138) predicts that the minimum occurs for $S_1 \approx (4/7)/(2\pi S_2)$. It is instructive to analyze how the depth of the minimum varies with counterion valency at high charge density. Using eq.(136) and neglecting logarithmic terms we find that in the minimum, $A(h_{min})/kT \approx -\frac{7}{4}\sqrt{2\pi S_2}$ The minimum in free energy corresponds to the adhesion energy per counterion. The adhesion energy is typically measured per unit wall charge, which we obtain dividing by $Z/2$,

$$A_{adh}/kT \approx -7 l_B \sqrt{\frac{\pi Z \sigma}{2e}} \tag{139}$$

Thus, in the regime of strong electrostatic coupling, the adhesion energy is relatively weakly dependent on the counterion valency as well as on the surface charge density.

5.6 Experimental manifestations of ion-ion correlations

The theoretical discussion has shown that there is an attractive contribution to the force between two similarly charged surfaces or particles. This attraction is short ranged, it decays like h^{-3} for a saltfree planar double layer, and it is *e.g.* more significant the higher the valency of the counterion and the lower the dielectric permittivitty. It is typically stronger than the van der Waals contribution. Experimentally, the effect can manifest itself as an unexpected attractive force or when the effect is less strong, as a substantial weakening of the repulsive double layer force.

There exists several powerful methods for measuring repulsive forces, while it is much more difficult to measure an attraction, because the system is then inherently unstable. In measurements one has either to balance the attractive force by a known stronger repulsive

force or, as in the Surface Force Apparatus (SFA) and the Atomic Force Microscopy, balance the attraction with a sufficiently stiff spring. Neither of these methods is easy to implement for strongly attractive forces and to our knowledge there is no clear-cut experimental measurement of attractive ion-ion correlation forces where one has been able to resolve the distance dependence of the force. On the other hand, there are numerous experiments indirectly demonstrating the existence of an attractive force that is most likely due to ion-ion correlations.

It is well established for many colloidal systems that di- and tri-valent ions can cause precipitation and/or coagulation. Such observations have usually been interpreted in terms of the DLVO theory even in cases where the quantitative description indicated a discrepancy between theory and experiment. One then concluded that the multivalent ions could form "salt bridges" or coordinate specifically between the surfaces. One common example is the precipitation of soaps by calcium or magnesium ions. It is not easy to separate one effect from the other and different conceptual descriptions in fact overlap. We argue, however, that when an attractive force is observed under conditions where the theory predicts an attraction, this is a strong indication that one has a manifestation of the effect.

One of the first clear experimental demonstrations of the correlation effect was in a study of the swelling of the lamellar liquid crystalline phase formed by the anionic surfactant AOT. With the normal counterion Na^+, the lamellar phase swells to ca 80 per cent water. This could be quantitatively modeled using the PB approximation, while with divalent counterions such as Ca^{2+} and Mg^{2+} a lamellar liquid crystalline phase was still formed, but it only incorporated around 40 per cent water. For the mixed ternary system NaAOT - CaAOT- water it was observed that at intermediate ratios there was a transition from strong to weak swelling and simultaneously a coexistence of two lamellar phases. Simulations predict that for monovalent ions there is a small correction to the PB approximation, while for divalent ions attraction dominates - see Fig.33. Furthermore, in the transition from attraction to repulsion the force curve shows a non-monotonic behavior on the repulsive side, see Fig.38. This means that two lamellar phases are co-existing. It is interesting to note that the phase separation occurs with a force that is net repulsive at all separations. It is often stated that one needs an attractive region in the force to cause phase separation, but a non-monotonic repulsive force is in fact sufficient.
Experimental studies of electric double layers at mica surfaces in the presence of trivalent counterions has found a *charge inversion* of the mica surfaces, which is yet another manifestation of ion-ion correlations.

Above we have concentrated on forces between planar, or nearly planar, surfaces. The first explicit discussion of attractive ion-ion correlation forces due to Oosawa, was inspired by experiments in polyelectrolyte systems. In this case the basic models assume a cylindrical geometry. As discussed above there is for these types of systems numerous examples where the addition of divalent and trivalent counterions induce precipitation, but it is difficult to separate the role of short range interactions from the typical ion-ion correlation effects operating at a slightly longer range. So far the most studied cases are DNA and virus systems where the coil-globule transition can be caused by both multivalent counterions and by lowering of the solvent dielectric permittivity see Fig. 39.
Salt effects on ion-ion correlation can be quite spectacular. In a system with multivalent

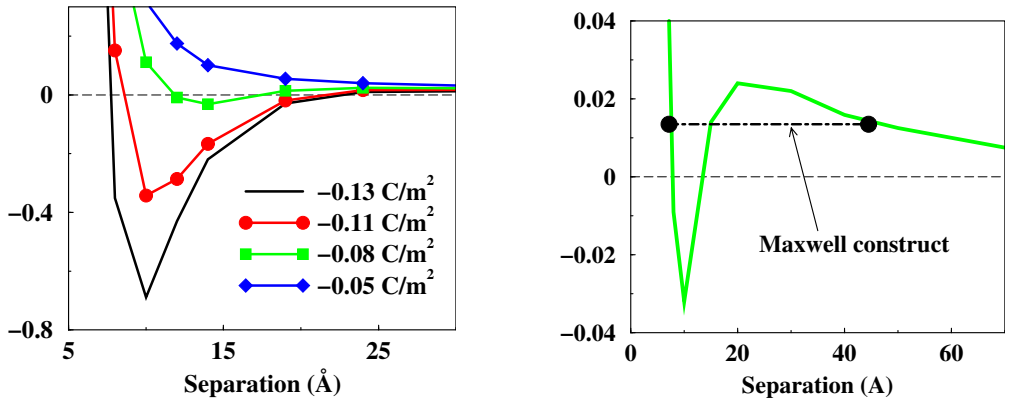

Figure 38: a) The electrostatic component of the osmotic pressure as a function of separation for a system with divalent counterions. The bulk solution consists of pure water; *i.e.* $p_{osm}^{bulk} = 0$ and the surface charge density is indicated in figure. b) The pressure as a function of separation with $\sigma = -0.08$ C/m^2. The two stable separations are shown as black spheres and connected with a dot-dashed line. Bjerrum length of 7.14 Å are used.

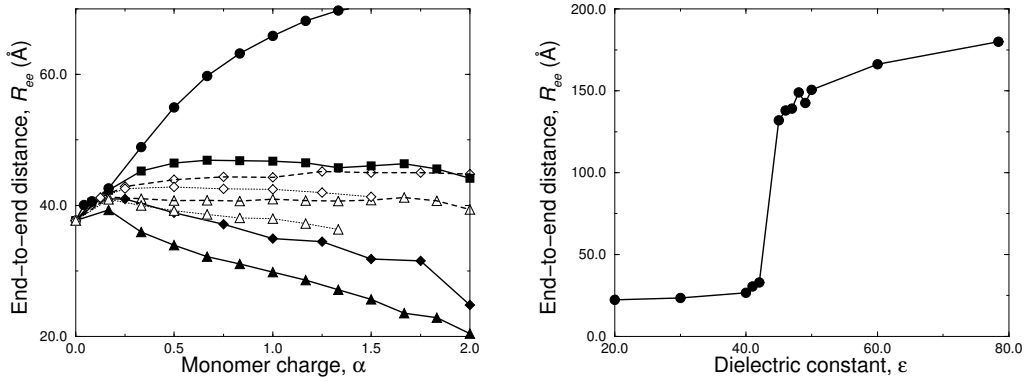

Figure 39: a) The end-to-end distance of a 24 monomer polyelectrolyte as a function of monomer charge. In the Monte Carlo simulations different counterions have been used. Solid lines are for point counterions, dashed lines are for oligo-electrolytes (connected monovalent ions) with bond length=6 Å and the dotted lines are for oligo-electrolytes with bond length=4 Å. The valencies of the counterions are: circles-monovalent, squares-divalent, diamonds-trivalent and triangles-tetravalent. b) The end-to-end distance of a 60 monomer polyelectrolyte as a function of the dielectric constant. Here the monomer charge is fixed to -1 and simple monovalent counterions are used.

counterions and low salt content attractive forces will dominate. Upon addition of a 1:1 salt, there will be a competition between the original multivalent counterions and the monovalent ones coming from the salt. At sufficiently high salt concentration the attraction can disappear and the system will revert to a "normal" double layer repulsion. Thus, we have the unexpected situation that addition of salt leads to *increased* repulsion. The phenomenon can be observed in dilute DNA solutions, where initially compacted DNA (by spermidine or spermine) expands if the salt concentration becomes sufficiently high - see Fig. 40.
For spherical particles it has turned out to be more difficult to find clear demonstrations of the ion-ion correlations. For a given charge density, the electrostatic interactions are weaker between spheres than between planes as, for example, can be seen from the Derjaguin approximation. Consequently, one needs a higher charge density in the spherical system relative to the planar or cylindrical cases in order to see a net attraction. Furthermore, if one uses multivalent counterions, one easily reaches the precipitation limit, where the physical origin of the observed effect is less clear.

5.7 Polyelectrolyte effects on the double layer repulsion

The addition of flexible polyelectrolytes to a charged colloid has a strong impact on the intercolloidal force and can cause both a stabilization and destabilization of the colloid. This is used in many technical applications, *e.g.* in pulp production, food industry and water refinement to mention a few. Biological systems also contain flexible polyelectrolytes, such as spermine and spermidine for "packing" of DNA and polyelectrolytes also appear in the blood coagulation process and as glycolipids at membrane surfaces.

The force behaviour in the presence of polyelectrolytes is diverse and we can not expect the simple Poisson-Boltzmann equation to explain the experimental observations. In fact a large variety of "non-DLVO" behaviour is seen in such systems. We will here discuss a few idealized situations using a simplified polymer model, which however retains two important properties - connectivity and flexibility. These are of special importance when polyelectrolytes interact with charged surfaces and modulate their interaction.

Consider a simple double layer system where the interaction between two charged surfaces is strongly repulsive. Now convert the counterions into polyelectrolyte chains by connecting them with harmonic bonds as depicted in Fig.41. One can imagine three distinct situations with:

- A fraction of counterions is connected giving an "undercompensated system".
- All counterions are transformed into polyelectrolyte chains, giving a "perfectly matched" system.
- Extra salt is added and some of these ions are connected as well, giving an "overcompensated" system.

In the perfectly matched system, one finds that the original double layer repulsion has completely disappeared and a very strong attraction appears at short separation see Fig.42. The extra attraction comes from a bridging of polyelectrolyte chains at short separation. The driving force for the bridging is a gain in chain entropy. At large surface-surface

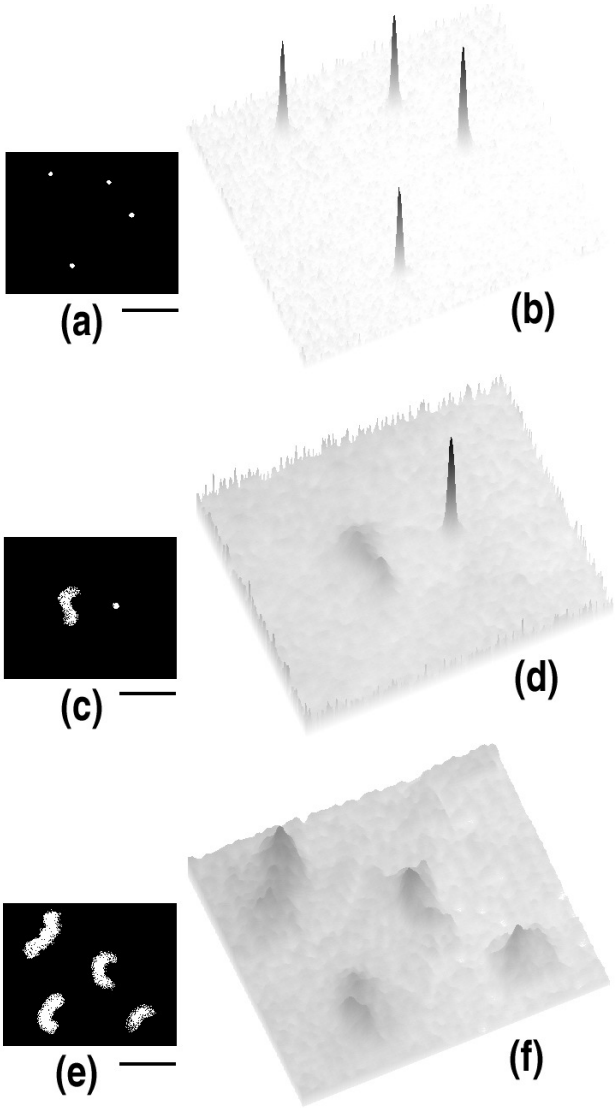

Figure 40: Experimental evidence that simple salt unfolds DNA compacted by spermine. a), c) and e) are video frames from the fluorescence microscopy image of single T4 DNA molecules at [spermine]=2.0×10^{-6} M. The scale bar represents 5 μm. b), d) and f) are the corresponding quasi-three-dimensional representations of the fluorescence intensity. a) and b) shows the salt-free case, [NaCl]=0, where the DNA molecules exhibit a globular conformation. In c) and d), [NaCl]=30 mM, the DNA molecules coexist in both elongated coiled and compacted globular structures. For high salt concentrations, [NaCl]=300 mM, all DNA molecules have a coiled structure.

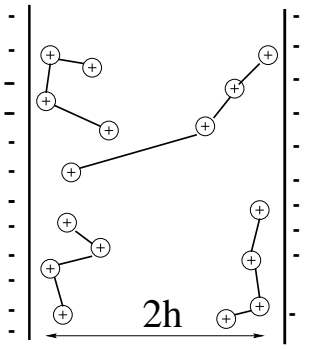

Figure 41: Schematic picture of an electric double layer with neutralizing polyelectrolyte counterions.

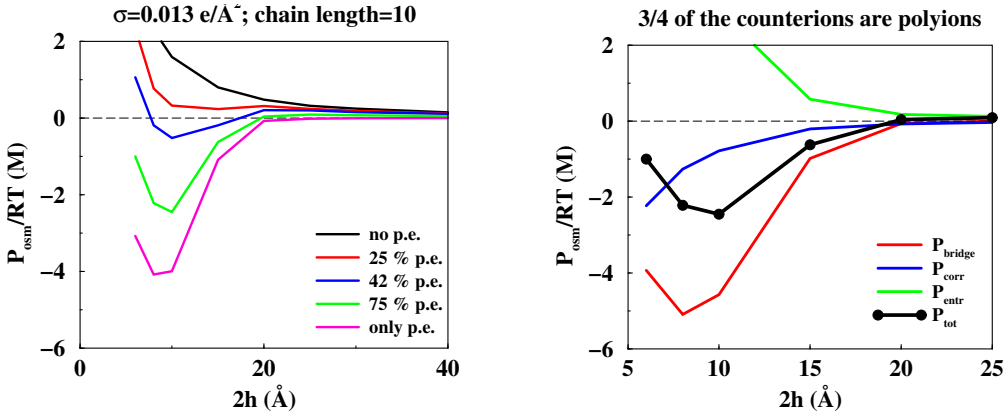

Figure 42: a) The osmotic pressure in an electrical double layer system with varying amount of polyelectrolytes. The yellow curve is a perfectly matched system, while the others represent different degrees of undercompensation. b) The magnitude of the different pressure components of eq.(140) for an undercompensated system.

separation the chains are confined to their respective surfaces with a comparatively low chain entropy. When the separation decreases and becomes of the order of the monomer-monomer distance, then the chains can, at a small electrostatic cost, bridge over to the other surface and thereby substantially increase the chain entropy.

The osmotic pressure can be determined via the so-called contact theorem, *cf.* eq.(115). For a polyelectrolyte system the contact relation should be modified to include also a bridging term,

$$p_{osm} = kTc(h) - \frac{\sigma^2}{2\epsilon_r\epsilon_0} \qquad p_{osm} = kTc(0) + p^{corr} + p^{bridge} \tag{140}$$

Fig.42b shows a comparison of the entropic term, $kTc(0)$, and the attractive terms as a function of separation. The position of the force minimum is found at distance approximately equal to the monomer-monomer separation and the magnitude varies approximately as the inverse square of the monomer-monomer separation.

Up to now the focus has been on theoretical results and it seems legitimate to ask whether they are directly reproduced experimentally. Fig.43 shows a surface force experiment with 10^{-4} M KBr in one experiment and the addition of a polyelectrolyte in another. The polyelectrolyte addition completely wipes out the double layer repulsion and an attraction appears at about 100 Å.

Increasing the salt concentration to 10^{-2} M makes the double layer repulsion appear again. The result can be interpreted as due to an increased adsorption at high salt concentration. The salt screens the repulsion between the polyelectrolyte charges and the charged walls adsorb more chains than necessary for neutralization and a charge reversal appears. This is an overcompensated system. Similarly, a repulsion can also appear if the amount of polyelectrolyte adsorbed is significantly less than what is required for neutralization - see Fig.42a. In both cases we will find something that resembles ordinary double layer repulsion. In fact, it is only fairly close to a perfect match, that the double layer completely disappears.

In a double layer system with monovalent counterions, the addition of salt will always lead to a decreased repulsion. In a polyelectrolyte system, however, the opposite is possible,

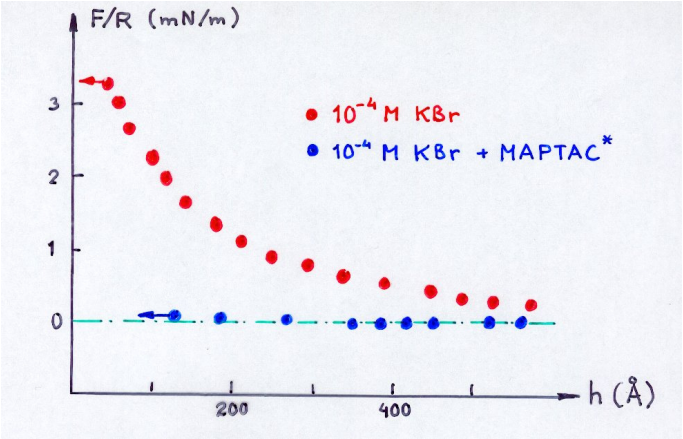

Figure 43: The interaction of two negatively charged mica surfaces in 10^{-4} M KBr (red symbols) and with the addition of a cationic polyelectrolyte ,MAPTAC= $[\text{-CH}_2\text{-CCH}_3\text{-CO-NH-(CH}_2)_3\text{-N}^+(\text{CH}_3)_3]_n$, (blue symbols).

since the salt concentration will directly affect the amount of adsorbed polyelectrolyte as well as its configuration. The addition of salt to a polyelectrolyte system also has a more subtle effect, since it affects the so-called Donnan equilibrium.

6 Polymer Induced Forces - *preliminary*

6.1 A free polymer

Let us start by consider a free polymer(ideal), sometimes refered to as a freely jointed chain. Following Israelachvili we denote the number of polymers by n and the monomer-monomer separation by l. The end-end separation is then given by

$$R_{ee} = \sqrt{n-1}l \tag{141}$$

A more common, and experimentally accessible quantity, is the radius of gyration,

$$R_g^2 = \frac{\sum_{i=1}^{n}\sum_{j=1}^{n}(\mathbf{r}_i - \mathbf{r}_j)^2}{2n^2} = \frac{\sum_{i=1}^{n}(\mathbf{r}_i - \mathbf{r}_{com})^2}{n} \tag{142}$$

We can also derive explicit expressions for the freely jointed chain,

$$R_g^2 = \frac{(n-1/n)}{6}l^2 \approx \frac{nl^2}{6} \tag{143}$$

and by combining this with eq.(141) we get,

$$R_g^2 = \frac{1+1/n}{6}R_{ee}^2 \approx \frac{R_{ee}^2}{6} \tag{144}$$

These relations are for an ideal or a chain in a so called *theta solvent*. For a *bad* or a *good* solvent the radius of gyration will be different and Israelachvili then uses the word *Flory radius* for R_g in a real solvent. He also introduces an expansion factor,

$$R_F = R_g^{real} = \alpha R_g^{ideal} \tag{145}$$

The expansion factor can be both smaller and larger than unity. In a good solvent it will be larger than one and the chain will expand like,

$$R_F = n^{3/5}l \tag{146}$$

This relation is derived under the assumption that there is a short range repulsion between the monomers. The chain will scale differently with n depending on the interaction between the monomers and below follow a collection of different behaviours:

- Attractive interactions $R_{ee} \sim n^{1/3}l$
- Ideal chain $R_{ee} \sim n^{1/2}l$
- Short range repulsion $R_{ee} \sim n^{3/5}l$
- Polyelectrolyte in salt solution $R_{ee} \sim \kappa^{-2/5}n^{3/5}l$
- Polyelectrolyte in infinite dilution $R_{ee} \sim nl$

6.2 Polymers at surfaces

Polymers can act as both stabilizers and coagulants, that is they can give rise to both repulsive and attractive interactions between macromolecules. Polymers can be attached to surfaces by direct adsoprtion, by covalent linkage(expensive) or by block adsorption. Non-adsorbing polymers can also affect the force and this we will discuss in terms of depletion attraction.

We will focus on neutral polymers and leave out polylectrolytes and polyampholytes, which of course also are very important. The simplest case is with end-grafted chains at low surface coverage, Γ. For separations $2R_g < D < 8R_g$ one can describe the energy of interaction with,

$$\beta W_S(D) = 36\Gamma \exp(-D/R_g) \tag{147}$$

If the amount of polymer increases then the behaviour becomes more complex, since the chain starts to expand and the thickness of the adsorbed layer, L, in a good solvent can be approximated by,

$$L = \Gamma^{1/3} R_F^{5/3} \approx \Gamma^{1/3} nl \tag{148}$$

that is, the full length of the polymer. Alexander-deGennes have derived an expression for the pressure

$$\beta p_A(D) = \Gamma^{3/2}[(\frac{2L}{D})^{9/4} - (\frac{D}{2L})^{3/4}] \tag{149}$$

Eq.(149) is valid for $D < 2L$ and it can be further simplified if $0.4L < D < 1.8L$,

$$\beta p_A(D) = 100\Gamma^{3/2} \exp(-\pi D/L) \quad \text{and} \quad \beta W_A(D) = \frac{100L}{\pi}\Gamma^{3/2} \exp(-\pi D/L) \tag{150}$$

We may rewrite eqs.(147) and (150) in terms of n and l in order to facilitate their comparison. Then we obtain the following expressions,

$$\beta W_S(D) = 36\Gamma \exp(-\sqrt{6}D/\sqrt{n}l) \tag{151}$$

$$\beta W_A(D) = \frac{100nl^{5/3}}{\pi}\Gamma^{11/6} \exp(-\pi\Gamma^{1/3}D/nl^{5/3}) \tag{152}$$

The important point to note is that the good solvent case gives a much more long ranged steric repulsion.

It turns out that this Alexander-deGennes theory fits experimental data very well - see figs. 14.3 and 14.4 in Israelachvili. Discuss fig. 14.6 as a comparison between a surface with needles and a surface with chewing gum. Discuss the term bridging.

6.2.1 Depletion forces

A very important mechanism of polymer interaction is the depletion force. This means that when two surfaces come close then the polymer can not fit into the intervening slab, but is excluded from the space and we get a negative pressure. The interaction sets in at approximately $D \approx R_g$. This means that the range increases with $\sqrt{n}$.

One can show that for long chains the pressure is given as,

$$\frac{p}{p_{bulk}} = \frac{8}{\pi^2}\sum_{j=1}^{\infty} \exp(-((2j-1)\pi/Z)^2)[\frac{1}{(2j-1)^2} + \frac{2\pi^2}{Z^2}] \tag{153}$$

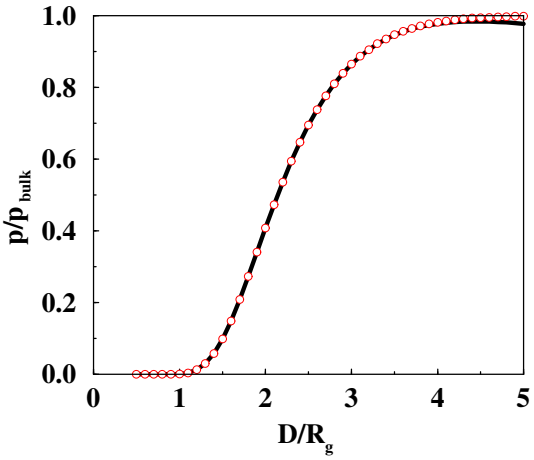

Figure 44: The depletion pressure for an ideal infinitely long chain. See equations above.

where $Z = h/R_g$. In fact, it is enough to incorporate only the first term in eq.(153) and we can write the pressure as,

$$\frac{p}{p_{bulk}} = \frac{8}{\pi^2}\exp(-2\pi/z^2)(1+\frac{2\pi^2}{Z^2}) \tag{154}$$

Fig. 44 shows the pressure evaluated with the first two terms of the sum in eq.(153).